A general and explicit Eshelby-type estimator for evaluating the equivalent stiffness of multiply coated ellipsoidal heterogeneities

Akbar Ghazavizadeh, Mohamed Haboussi, Akrum Abdul-Latif, Akbar Jafari, Houssem Bousoura

A general and explicit Eshelby-type estimator for evaluating the equivalent stiffness of multiply coated ellipsoidal heterogeneities

Akbar Ghazavizadeh [a,b*] , Mohamed Haboussi [c], Akrum Abdul-Latif [b], Akbar Jafari [d]

[a] LABEX SEAM - Université Paris 13, Sorbonne Paris Cité, avenue Jean-Baptiste Clément, 93430, Villetaneuse, France

[b] Laboratoire Quartz, Supméca, 3, rue Fernand Hainaut, 93407 St Ouen Cedex, France

[c] Université Paris 13, CNRS, UPR3407, LSPM, Sorbonne Paris Cité, avenue Jean-Baptiste Clément, 93430, Villetaneuse, France

[d] Department of Mechanical Engineering, Sirjan University of Technology, Sirjan, Iran, POBOX 7813733385

[*]Corresponding author: akbar.ghazavizadeh@univ-paris13.fr- Tel: +33 (0)6 17 27 08 57

Co-author: mohamed.haboussi@lspm.cnrs.fr - Tel: +33 (0)1 49 40 34 70

Co-author: aabdul@iu2t.univ-paris8.fr – Tel: +33 (0)1 41 51 12 34

Co-author: jafari@sirjantech.ac.ir – Tel: +98 (0)34 55 20 20 11

A general and explicit Eshelby-type estimator for evaluating the equivalent stiffness of multiply coated ellipsoidal heterogeneities

Abstract

The paper presents an efficient estimator for the equivalent stiffness calculation of multiphase ellipsoidal heterogeneities. This estimator is derived from the exact effective stiffness of a generic monofiller composite associated with Eshelby's equivalence principle. It is originally developed for a two-phase ellipsoidal configuration and is subsequently generalized to multiphase heterogeneities via a layer-wise sweeping procedure. The developed estimator has an explicit form, which makes it amenable to computer programming. The performance of the proposed estimator is evaluated by analyzing several numerical examples of spherical compounds and two spheroidal ones spanning a wide range of elasticity contrasts, which are also examined by two other applicable Eshelby-type estimators. To assess the validity of our estimator in two-level homogenization problems, several examples of composite systems reinforced with core-shell inclusions are analyzed using a two-level homogenization scheme in which use is made of the estimator of this study. It is concluded that the presented estimator can be applied to a wide range of multiphase ellipsoidal heterogeneities or limit cases thereof, as well as heterogeneities with radially graded interphases.

Keywords: Equivalent inhomogeneity/effective particle; multicoating inclusion; Eshelby-type estimators; radially graded interphase; two-level homogenization; spherical core/shell compounds.

1. Introduction

EQUIVALENT INHOMOGENEITY, also referred to as effective particle in the literature on the homogenization of heterogeneous solids, is understood as a homogeneous replacement for a locally inhomogeneous domain [1–8]. This concept is particularly

applicable to particulate and fiber composites containing singly or multiply coated reinforcements. A coating might be simply the interfacial transition zone, also known as the interphase layer, which is formed around fillers and possesses properties most likely different from the host matrix. In this case, the interphase layer serves as an intermediate between the matrix and fillers through which load transfer (mechanical, thermal, etc.) takes place. For the overall properties homogenization of such composite systems where multiphase particles are suspended in a homogeneous continuum, a two-level homogenization scheme is usually implemented as a judicious practice [3,9–11] in order to simplify to a great extent the usually complicated original problem of effective properties calculation to a small detriment of the exact results.

In two-level homogenization practices, the first estimation of effective properties is conducted at the level of multiphase heterogeneities, where appropriate estimators are employed to characterize the equivalent homogeneous replacement for the original compound filler. For the second level of homogenization, one will have homogeneous reinforcements already characterized at the first level, which are suspended in a continuous matrix identical with the original problem. This second homogenization part looks like a conventional overall properties calculation for which quite a few approaches are available from micromechanics of heterogeneous materials, such as [12,13]. Hence, breaking the homogenization analysis into two (or multiple) levels significantly reduces the complexity of the problem at the expense of losing some accuracy.

Equivalent properties of multiphase fillers are a function of the geometry and properties of the constituents as well as their relative position. In the present study, we propose a general estimator that enables the direct and efficient evaluation of the effective properties of multi-layered fillers of any material symmetry and any ellipsoidal geometry. The proposed estimator, called GEEE (General Explicit Eshelby-type Estimator), is in fact a mean-field, analytical, Eshelby-type estimator

that is derived from the seminal work of Eshelby [14]. For performance evaluation and comparison purposes, two other Eshelby-type estimators of Hori & Nemat-Nasser's Model (HNNM) [15] and modified HNNM [16], are also implemented and discussed. The versatility of the ellipsoidal configuration adopted in these methods allows covering a wide range of geometries often seen in practical and theoretical applications such as spheres, long cylinders and thin platelets. This quality gives Eshelby-type approaches an absolute advantage over non Eshelby-type ones. This latter class of analytical, mean-field homogenization estimators is indeed less general than Eshelby-type ones in terms of geometry and material symmetry as they are developed for specific configurations (i.e. combination of geometry & material symmetry of phases). Examples of this second class of approaches developed for spherical core/shell heterogeneities are Hashin's CSA (composite spheres assemblage) [17], Hervé & Zaoui's composite spheres model [18], Maxwell's estimator [19], polarization approximation [3] and annular coated inclusion (ACI) [20]. It is worth mentioning that in the terminology of this work and its sequels, the term "estimator" is reserved for referring to micromechanical methods that have been specifically developed for (such as GEEE) or can also be used for (such as HNNM) estimating the equivalent stiffness of multiphase heterogeneities.

In this study, we focus on the detailed presentation of a newly developed efficient estimator, namely GEEE. As will be shown subsequently, it has the advantage of possessing an explicit and easy-to-use expression, as opposed to the implicit and nonlinear equations of HNNM and modified HNNM. The easy-to-use estimator of this study, is an answer to the need recognized by Shen and Li [8], among others, that '*analytical results are limited for inhomogeneous interphases*' and that '*numerical procedures are usually utilized to solve governing differential equations*'. While being free from any kind of differential equation or complicated numerical procedures, GEEE is expressed as a tensor equation of explicit form that can be

directly and efficiently applied to multiphase core/shell ellipsoidal heterogeneities, including the ones with radially graded (inhomogeneous) interphases.

In studying the numerical examples, we confine our attention mainly to the case of spherical heterogeneities with a small digression to spheroidal ones, and in the future publications we will address long cylindrical and thin platelet compounds. Spherical geometry, as a limit case of an ellipsoid with identical axes, is a simple but not less important configuration, which is commonly used in theoretical and practical applications for approximating nearly isodimensional micro/nanoparticles. For example, Li, Zhao, Pang, & Li [21] used a three-component spherical core/shell model to build the "basic element" of concrete and study its overall elastic response. The core of their model corresponds to an aggregate in which the first shell copies the interphase around the aggregate and the second shell represents the cement paste. Odegard, Clancy, & Gates [22] used a spherical core/shell model to study the impact of the interphase layer around silica nanoparticles immersed in polyimide on the effective elastic properties. An identical model was employed in [23] to investigate the overall properties of particulate composites containing spherical heterogeneities with graded properties in their coating. Diani, Gilormini, Merckel, & Vion-Loisel [24] also used spherical core/shell arrays to model carbon black filled rubbers and studied the impact of the interphase layers around carbon black particles. Similar configurations have been adopted to study syntactic foams [25,26], the impact of inhomogeneous interfacial transition zone in concrete [27], the effective thermal properties of aluminum matrix composites loaded with coated diamonds [28], and microencapsulated phase change materials [29], to mention a few.

To assess the performance of our proposed estimator, GEEE, and compare it with other Eshelby-type estimators cited above, namely HNNM (Hori & Nemat-Nasser's Model [15]) and modified HNNM [16], several numerical examples of multiphase spherical heterogeneities composed of isotropic core/shell components of various stiffness contrasts are examined. In this regard, the estimators HNNM and

modified HNNM are specialized to multilayer spherical particles. To keep the manuscript sufficiently self-contained, the mathematical manipulations required to obtain the expressions of HNNM and modified HNNM are provided in Appendix A and Appendix B, respectively. The performance of the proposed GEEE in two-level homogenization problems is also evaluated by studying several composite systems reinforced with coated fillers.

Throughout this work, hollow, uppercase Roman letters denote fourth-order tensors. The inverse of the fourth-order tensor $\mathbf{A}$, for example, is indicated by $\mathbf{A}^{-1}$. Second-order tensors are represented in bold, lowercase, Greek letters. Italicized letters are reserved for scalar quantities. In tensor equations, the commonly used symbol ':' denoting the double contraction over the last two indices of the first tensor (multiplier) and the first two indices of the second tensor (multiplicand), is dropped for brevity. Finally, when required, numeral superscripts are placed between parentheses to avoid confusion with exponents.

The present investigation is organized as follows. Section 2 provides the details of the proposed estimator, GEEE by starting from the exact effective stiffness of a monofiller composite. Section 3 is devoted to the examination of relevant numerical examples of multiphase spherical particles whose results allow for evaluating the performance of each estimator. Concluding remarks are given in the last section. A brief derivation of more general bounds of Hashin-Shtrikman for the equivalent shear and bulk moduli of multiphase spherical particles is given in Appendix C.

2. GEEE: from 2-phase formulation to *n*-phase generalization

The General Explicit Eshelby-type Estimator (GEEE), which is derived in this section, is an efficient and easy-to-use Eshelby-type estimator that possesses an explicit equation in $\mathbf{C}^{eq}$, the equivalent stiffness of the composite heterogeneity. The derivation is split into two steps: formulation of GEEE for a generic two-phase

ellipsoidal heterogeneity, and then the generalization of 2-phase formulation to *n*-phase one through a recursive algorithm, which is subsequently mathematically demonstrated.

The 2-phase formulation of GEEE constitutes its back-bone and is directly derived from Eshelby's equivalence principle [30]. According to this principle, which is illustrated in Figure 1, an ellipsoidal heterogeneity in a homogeneous medium of large dimensions can be equally replaced by an inclusion of the same shape but of host medium material. To compensate for the material change between the heterogeneity and inclusion, a uniform transformation (free-stress) strain, denoted by $\boldsymbol{\varepsilon}^*$, is attributed to the inclusion. $\boldsymbol{\varepsilon}^*$ is determined such that under remote uniform loading on both systems, the elastic fields of the ellipsoidal regions are identical, thereby establishing the equivalence between both systems.

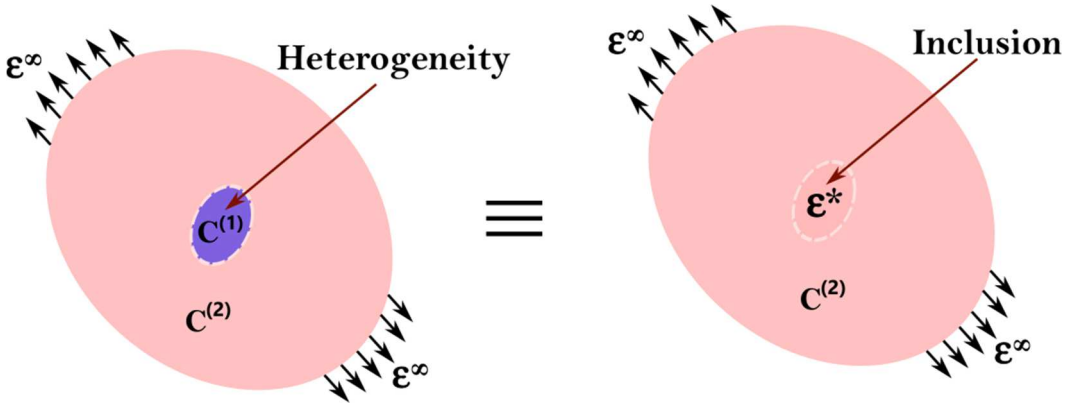

Figure 1. Monofiller composite illustration of Eshelby's equivalence principle: an ellipsoidal heterogeneity is suspended in a homogeneous matrix of large dimensions, which is subjected to uniform loading boundary conditions. In the equivalent system, the heterogeneity is replaced by an inclusion of matrix material in addition to an unknown transformation strain.

From the second system, the superposition of uniform remote strain, $\boldsymbol{\varepsilon}^{\infty}$, and the perturbation strain induced in the inclusion, $\boldsymbol{\varepsilon}^{p}$, due to $\boldsymbol{\varepsilon}^*$ corresponds the inclusion's strain, $\boldsymbol{\varepsilon}^{I}$.

$$\boldsymbol{\varepsilon}^{I} = \boldsymbol{\varepsilon}^{\infty} + \boldsymbol{\varepsilon}^{p} = \boldsymbol{\varepsilon}^{\infty} + \mathbf{S}\boldsymbol{\varepsilon}^{*} \tag{1}$$

The equation $\boldsymbol{\varepsilon}^{\mathrm{p}} = \mathbf{S}\boldsymbol{\varepsilon}^{*}$ is one of the results of Eshelby's problem. Another result is the expression of perturbation stress, $\boldsymbol{\sigma}^{\mathrm{p}} = \mathbf{C}^{(2)}\left(\mathbf{S}-\mathbf{I}\right)\boldsymbol{\varepsilon}^{*}$, induced in the inclusion due to $\boldsymbol{\varepsilon}^{*}$. Hence, the total stress of the inclusion is obtained from the superposition of $\boldsymbol{\sigma}^{\mathrm{p}}$ and uniform remote stress, $\boldsymbol{\sigma}^{\infty} = \mathbf{C}^{(2)}\boldsymbol{\varepsilon}^{\infty}$.

$$\boldsymbol{\sigma}^{\mathrm{I}} = \boldsymbol{\sigma}^{\infty} + \boldsymbol{\sigma}^{\mathrm{p}} = \mathbf{C}^{(2)}\left[\boldsymbol{\varepsilon}^{\infty} + \left(\mathbf{S}-\mathbf{I}\right)\boldsymbol{\varepsilon}^{*}\right] \tag{2}$$

Identity of the strains in the heterogeneity and inclusion allows for calculating $\boldsymbol{\sigma}^{\mathrm{H}}$, the stress inside the heterogeneity.

$$\begin{aligned} \boldsymbol{\varepsilon}^{\mathrm{H}} &= \boldsymbol{\varepsilon}^{\mathrm{I}} = \boldsymbol{\varepsilon}^{\infty} + \mathbf{S}\boldsymbol{\varepsilon}^{*} \\ \boldsymbol{\sigma}^{\mathrm{H}} &= \mathbf{C}^{(1)}\boldsymbol{\varepsilon}^{\mathrm{H}} = \mathbf{C}^{(1)}\left(\boldsymbol{\varepsilon}^{\infty} + \mathbf{S}\boldsymbol{\varepsilon}^{*}\right) \end{aligned} \tag{3}$$

Equality of stresses in both ellipsoidal regions, i.e. $\boldsymbol{\sigma}^{\mathrm{H}} = \boldsymbol{\sigma}^{\mathrm{I}}$, gives the sough-for unique $\boldsymbol{\varepsilon}^{*}$ that establishes the equivalence between both systems.

$$\boldsymbol{\sigma}^{\mathrm{I}} = \boldsymbol{\sigma}^{\mathrm{H}} \qquad \Rightarrow \qquad \boldsymbol{\varepsilon}^{*} = -\left[\left(\mathbf{C}^{(1)} - \mathbf{C}^{(2)}\right)^{-1}\mathbf{C}^{(2)} + \mathbf{S}\right]^{-1}\boldsymbol{\varepsilon}^{\infty} \tag{4}$$

Substitution of the above expression into relation (3), results in the following equation.

$$\boldsymbol{\varepsilon}^{\mathrm{I}} = \boldsymbol{\varepsilon}^{\mathrm{H}} = \left[\mathbf{I} + \mathbf{S}\left(\mathbf{C}^{(2)}\right)^{-1}\left(\mathbf{C}^{(1)} - \mathbf{C}^{(2)}\right)\right]^{-1}\boldsymbol{\varepsilon}^{\infty} \tag{5}$$

For ease of reference the concentration tensor behind $\boldsymbol{\varepsilon}^{\infty}$ in the above equation is hereafter denoted by $\mathbf{A}$. Thus far, no approximation has been made in deriving expression (5) that correlates the uniform strain of the heterogeneity to remote uniform strain imposed on the monofiller composite system. This implies that under the assumptions of Eshelby's problem and for the monofiller composite under study, $\mathbf{A}$ is exact.

Now, the average theorems are invoked to calculate mean overall strain and stress of the monofiller composite system from which its effective stiffness is determined. Denoting the average stress and strain of the matrix by the superscript $^{\mathrm{M}}$, the average theorems give

$$\begin{cases} \overline{\boldsymbol{\varepsilon}} = \boldsymbol{\varepsilon}^{\infty} = f_{\mathrm{H}}\overline{\boldsymbol{\varepsilon}}^{\mathrm{H}} + (1-f_{\mathrm{H}})\overline{\boldsymbol{\varepsilon}}^{\mathrm{M}} \;\Rightarrow \\ \overline{\boldsymbol{\sigma}} = \mathbf{C}^{\mathrm{eff}}\overline{\boldsymbol{\varepsilon}} = f_{\mathrm{H}}\overline{\boldsymbol{\sigma}}^{\mathrm{H}} + (1-f_{\mathrm{H}})\overline{\boldsymbol{\sigma}}^{\mathrm{M}} \Rightarrow \end{cases} \qquad \begin{cases} \overline{\boldsymbol{\varepsilon}}^{\mathrm{M}} = \dfrac{1}{1-f_{\mathrm{H}}}\left[\mathbf{I} - f_{\mathrm{H}}\mathbf{A}\right]\boldsymbol{\varepsilon}^{\infty} \\ \mathbf{C}^{\mathrm{eff}}\overline{\boldsymbol{\varepsilon}} = f_{\mathrm{H}}\mathbf{C}^{(1)}\overline{\boldsymbol{\varepsilon}}^{\mathrm{H}} + (1-f_{\mathrm{H}})\mathbf{C}^{(2)}\overline{\boldsymbol{\varepsilon}}^{\mathrm{M}} \end{cases} \tag{6}$$

$$\Rightarrow \qquad \mathbf{C}^{\mathrm{eff}} = \mathbf{C}^{(2)} + f_{\mathrm{H}}\left(\mathbf{C}^{(1)} - \mathbf{C}^{(2)}\right)\mathbf{A}$$

Here, $f_{\mathrm{H}} = V_{\mathrm{H}}/V_{\mathrm{tot}}$ is the volume fraction of the heterogeneity with respect to the entire monofiller composite. The expression of $\mathbf{C}^{\mathrm{eff}}$ is the result of Eshelby's equivalence principle and average theorems for the monofiller composite under consideration. This expression contains no approximate assumptions for the composite system made of a host matrix of large dimensions encapsulating a single ellipsoidal filler. Hence, for such a composite system, the above $\mathbf{C}^{\mathrm{eff}}$ is the exact description of its effective stiffness. In the following, we rely on two equivalent monofiller composites that are differently represented and then equate their exact $\mathbf{C}^{\mathrm{eff}}$ to obtain the expression of GEEE for a two-phase ellipsoidal inhomogeneity. This expression corresponds to the first part of GEEE, which is completed once it is generalized to *n*-phase heterogeneity.

2.1 Two-phase formulation of GEEE

Let an arbitrary ellipsoidal heterogeneity of stiffness $\mathbf{C}^{(1)}$ be embedded in a large host medium of elasticity $\mathbf{C}^{(2)}$ with perfect bonding conditions, as illustrated schematically in Figure 2. Complying with the conditions of monofiller composite of Eshelby's equivalence principle, its effective stiffness, $\mathbf{C}_{\mathrm{A}}^{\mathrm{eff}}$, is given by Eq.(6).

$$\mathbf{C}_{\mathrm{A}}^{\mathrm{eff}} = \mathbf{C}^{(2)} + f_1\left\{\left(\mathbf{C}^{(1)} - \mathbf{C}^{(2)}\right)\mathbf{A}^{(1)}\right\} \qquad \text{where} \quad \mathbf{A}^{(1)} = \left(\mathbf{I} + \mathbf{S}^{(1)}\left(\mathbf{C}^{(2)}\right)^{-1}\left(\mathbf{C}^{(1)} - \mathbf{C}^{(2)}\right)\right)^{-1} \tag{7}$$

In the same problem, any imaginary ellipsoidal region from the matrix material around the reinforcement can be treated as a coating with perfect bonding to both reinforcement and the rest of the matrix. Accordingly, in connection with Figure 2A, the heterogeneous system composed of a coated ellipsoidal heterogeneity embedded in a host matrix that shares the same elasticity with the coating, has an effective

stiffness that is expressed by Eq.(7). Now, the reinforcement plus its coating in problem (A) is replaced by an equivalent inhomogeneity of the same shape and orientation, as schematically illustrated in Figure 2B. In this new problem (B), the properties and dimensions of the host matrix beyond the coating remain unchanged. The configuration of problem (B) obviously fits the monofiller composite of Eshelby's equivalence principle in the same way that problem (A) does. Therefore, its effective stiffness is calculable similar to Eq.(7).

$$\mathbf{C}_{\mathrm{B}}^{\mathrm{eff}} = \mathbf{C}^{(2)} + f_{\mathrm{eq}}\left\{\left(\mathbf{C}^{\mathrm{eq}} - \mathbf{C}^{(2)}\right)\mathbf{A}^{\mathrm{eq}}\right\} \qquad \text{where} \qquad \mathbf{A}^{\mathrm{eq}} = \left(\mathbf{I} + \mathbf{S}^{\mathrm{eq}}\left(\mathbf{C}^{(2)}\right)^{-1}\left(\mathbf{C}^{\mathrm{eq}} - \mathbf{C}^{(2)}\right)\right)^{-1} \tag{8}$$

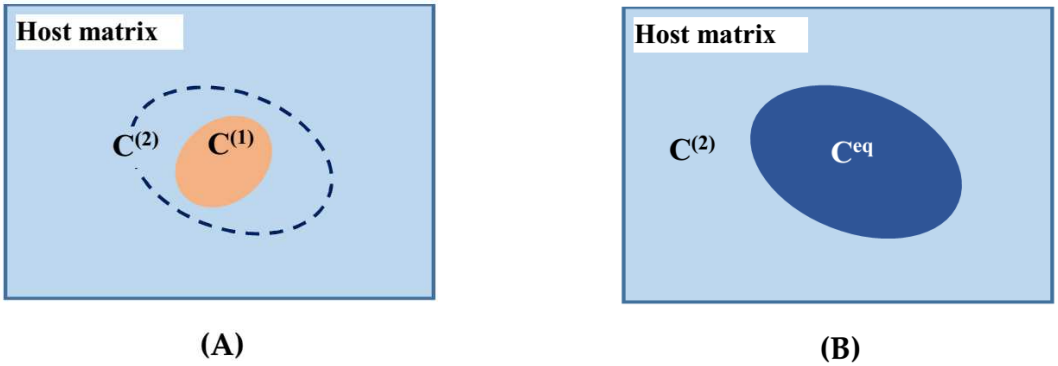

(A) **(B)**

Figure 2. Schematic of (A) an ellipsoidal heterogeneity embedded in a host medium of large dimensions. An ellipsoidal region from the host material is assumed encapsulating the heterogeneity; (B) The ellipsoidal heterogeneity together with its coating is replaced with a homogeneous inhomogeneity such that the overall elasticity of the original problem remains unchanged.

In problem (B), the elasticity of the equivalent inhomogeneity, $\mathbf{C}^{\mathrm{eq}}$, is unknown whereas its volume fraction, f_{eq}, and Eshelby's tensor, $\mathbf{S}^{\mathrm{eq}}$, are known because its dimensions and orientation are known beforehand. Equivalence between both configurations requires that $\mathbf{C}_{\mathrm{B}}^{\mathrm{eff}} = \mathbf{C}_{\mathrm{A}}^{\mathrm{eff}}$ from which, $\mathbf{C}^{\mathrm{eq}}$ is calculated as follows.

$$\mathbf{C}^{\mathrm{eq}} = \mathbf{C}^{(2)} + \nu_1\mathbf{C}^{(2)}\left[\mathbf{C}^{(2)} + \left(\mathbf{C}^{(1)} - \mathbf{C}^{(2)}\right)\left(\mathbf{S}^{(1)} - \nu_1\mathbf{S}^{\mathrm{eq}}\right)\right]^{-1}\left(\mathbf{C}^{(1)} - \mathbf{C}^{(2)}\right) \tag{9}$$

Here, $\nu_1 = f_1/f_{\mathrm{eq}} = V_1/V_{\mathrm{eq}}$ denotes the volume fraction of the core inclusion relative to the entire two-phase heterogeneity composed of the inclusion plus its coating. It is worth noting that although $f_1 = V_1/V_{\mathrm{tot}} \to 0$ and $f_{\mathrm{eq}} = V_{\mathrm{eq}}/V_{\mathrm{tot}} \to 0$, because the dimensions of the monofiller composites are sufficiently large, their ratio does not,

$f_1/f_{\text{eq}} = V_1/V_{\text{eq}} \not\to 0$. Also note that when $\mathbf{S}^{\text{eq}} = \mathbf{S}^{(1)}$, one retrieves Mori-Tanaka estimate of the effective stiffness of a two-phase composite consisting of aligned ellipsoidal heterogeneities of stiffness $\mathbf{C}^{(1)}$ and volume fraction v_1 dispersed in a matrix of stiffness $\mathbf{C}^{(2)}$.

The expression (9) is directly obtained from the exact solutions of the effective stiffnesses of two equivalent composite systems compatible with dilute configuration of Eshelby problem, hence $\mathbf{C}^{\text{eq}}$ of (9) is exact too for the configuration considered. Given that the terms on the right-hand side of (9) are not functions of $\mathbf{C}^{\text{eq}}$, this equation is explicit and no sophisticated numerical method is required for its solution. To exploit this equation, one has to calculate the associated Eshelby's tensors of ellipsoidal regions in advance. A major assumption is made here that this expression is equally valid when the two-phase heterogeneity is embedded in a different matrix. As will be discussed further below, with this simplifying assumption, the results of many estimators turn out to either coincide or be close to GEEE outputs. Besides, for several numerical examples we analyzed using GEEE in a two-level homogenization, a satisfactory agreement is observed between thus-calculated effective properties and the corresponding reference values from finite element analysis or the ACI model predictions.

For later reference, the definition of $\mathbf{C}^{\text{eq}}$ based on the average strains in the core and coating are also given below.

$$v_1\mathbf{C}^{(1)}\overline{\boldsymbol{\varepsilon}}^{(1)} + (1-v_1)\mathbf{C}^{(2)}\overline{\boldsymbol{\varepsilon}}^{(2)} = \mathbf{C}^{\text{eq}}\left[v_1\overline{\boldsymbol{\varepsilon}}^{(1)} + (1-v_1)\overline{\boldsymbol{\varepsilon}}^{(2)}\right] \tag{10}$$

The above definition of $\mathbf{C}^{\text{eq}}$ is invoked in the following subsection when generalizing GEEE to multiphase ellipsoidal heterogeneities. Although average strains appear in the above expression, $\mathbf{C}^{\text{eq}}$ defined as a property, is independent of the elastic fields of the ellipsoidal regions.

Remarks:

- A quick check reveals that the effective stiffness equation derived in (6) is essentially identical with Eshelby's dilute homogenization formulation. It has been discussed that Eq.(6) is an exact description of the effective stiffness of the monofiller composite explained earlier. However, in the literature when it is stated that Eshelby's dilute homogenization scheme is suitable for composites of dilute concentration, the volume fraction f_{H} is split over several fillers that are dispersed in a large host matrix. In this case, Eq.(6) gives only an approximation to the effective stiffness of multifiller composite, in that the filler-filler interactions are neglected. Naturally, the higher the volume fraction of fillers in the composite, the more pronounced the impact of inter-filler interactions will be, hence the more inaccurate the effective stiffness of the whole composite is identified by Eq.(6).

- After some mathematical manipulations, one can rewrite Eq.(9) in the following form.

$$\mathbf{C}^{\mathrm{eq}} = \mathbf{C}^{(2)} + \nu_1 \left[\left(\mathbf{C}^{(1)} - \mathbf{C}^{(2)} \right)^{-1} + \left(\mathbf{S}^{(1)} - \nu_1 \mathbf{S}^{\mathrm{eq}} \right) \left(\mathbf{C}^{(2)} \right)^{-1} \right]^{-1} \tag{11}$$

Since the reference stiffness of both ellipsoidal regions is $\mathbf{C}^{(2)}$, the products of Eshelby's tensors and the reciprocal of the reference stiffness are replaced with their corresponding polarization tensors. Therefore,

$$\mathbf{C}^{\mathrm{eq}} = \mathbf{C}^{(2)} + \nu_1 \left[\left(\mathbf{C}^{(1)} - \mathbf{C}^{(2)} \right)^{-1} + \mathbf{P}^{(1)} - \nu_1 \mathbf{P}^{\mathrm{eq}} \right]^{-1} \tag{12}$$

The advantage of this form of representation is that it clearly shows that $\mathbf{C}^{\mathrm{eq}}$ is always symmetric, no matter how the ellipsoidal regions are oriented with respect to one another, because the stiffness tensors and polarization tensors are always symmetric. In programming applications, however, the original expression of (9) is preferable as one single matrix inversion operation is involved whereas Eq.(12) contains two matrix inversions.

- It is instructive to note that in the derivation procedure, no constraint whatsoever has been placed on the volume fractions and no singularity due to volume fractions is possible in the formulation of GEEE. With regard to the extreme case of $\nu_1 \to 0$, the expression of Eq.(12) readily shows that $\mathbf{C}^{eq} \to \mathbf{C}^{(2)}$. On the other hand, when $\nu_1 \to 1$, it implies that the core and shell regions geometrically approach one another, hence $\mathbf{P}^{(1)} \to \mathbf{P}^{eq}$, and as a result $\mathbf{P}^{(1)} - \nu_1 \mathbf{P}^{eq} \to \mathbf{0}$. In this case, the expression of Eq.(12) suggests that $\mathbf{C}^{eq} \to \mathbf{C}^{(1)}$. Both limit values agree perfectly with the physical significance of the problem. Therefore, extreme volume fractions pose no problem to the implementation of GEEE and it works just as well as it does for intermediate volume fractions.

- Eq.(9), which is the core of GEEE, is presented in tensorial form, indicating that the impact of the relative orientation of phases and their material symmetry are automatically taken into account, as all tensorial quantities ought to be expressed in the same reference frame. In addition, Eshelby's tensors (or equivalently, the polarization tensors) take care of the effect of geometry (shape) of the phases. Therefore, the tensorial expression of Eq.(9) and Eshelby's tensors guarantee that relative orientations, material symmetries and the geometry of phases are taken into account.

- In analogy with the derivation of Eq.(9), one can independently derive the equivalent compliance of the core-shell configuration of interest by following a similar formalism but this time, under the stress applied conditions and prescribed transformation stress (eigenstress) instead of transformation strain (eigenstrain). The mathematical operations are straightforward using the discussions of § 7.3.2 - 7.3.4 of the textbook of Nemat-Nasser & Hori [12] and are not given here. After some mathematical manipulations, one can easily show that thus-calculated equivalent compliance and $\mathbf{C}^{eq}$ of Eq.(9) are each other's inverse, which indicates that GEEE satisfies the consistency condition.

- For a statistically homogeneous, two-phase, particulate composite in which inclusions are aligned in the matrix, Hashin-Shtrikman estimate of the effective stiffness derived by Ponte Castañeda and Willis [31] matches Eq.(12). Such a remarkable coincidence is more interesting when one notices that Eq.(12) is obtained as an equivalent stiffness estimator for ellipsoidal compounds whereas H-S estimate of [31] is derived based on the Hashin-Shtrikman variational structure developed by [32], and in the context of overall effective properties of particulate composites. As expounded by Ponte Castañeda and Willis [31], the H-S estimate is the lower (upper) bound of the composite effective stiffness should the matrix happen to possess the lowest (largest) stiffness moduli.

2.2 Generalization of 2-phase GEEE to *n*-phase heterogeneities

For ellipsoidal heterogeneities composed of $n > 2$ phases, Eq.(9) of GEEE obtained for two-phase heterogeneities shall be used n-1 times recursively to obtain the effective stiffness of the associated equivalent inhomogeneity. In the recursive application of Eq.(9), the underlying assumption is that $\mathbf{C}^{eq}$ of the n-phase heterogeneity is independent of the surrounding matrix and that each phase only *feels* the uniform elastic field of its immediate outer neighbor with the last coating assumed immersed in a matrix of its own properties. Consequently the strain of each phase directly depends on the uniform strain of its outer neighbor. Using these simplifying assumptions, one can readily calculate, in a layerwise manner as described below, the equivalent stiffness of the multiphase heterogeneity and subsequently the overall stiffness of the composite medium, knowing that the entire scheme will give rise to sort of numerically acceptable compromise on the final results.

Let an n-phase heterogeneity composed of a core inclusion encapsulated by n-1 layers, be entirely inserted in a homogeneous matrix, as schematized in Figure 3.

The objective is to establish a relationship between the equivalent stiffness of the *n*-phase compound and the *n*-1-phase sub-heterogeneity. To begin with, it is assumed that average strains $\overline{\boldsymbol{\varepsilon}}^{(1)}, \overline{\boldsymbol{\varepsilon}}^{(2)}, \ldots, \overline{\boldsymbol{\varepsilon}}^{(n)}$ are respectively induced in phase 1 (core), phase 2 (1st coating), …, phase *n* (outermost coating). Corresponding average stresses $\overline{\boldsymbol{\sigma}}^{(1)}$, $\overline{\boldsymbol{\sigma}}^{(2)}, \ldots, \overline{\boldsymbol{\sigma}}^{(n)}$ are also considered for each constituting phase. According to the average theorems, the average stress and average strain of the entire *n*-phase heterogeneity are defined as follows.

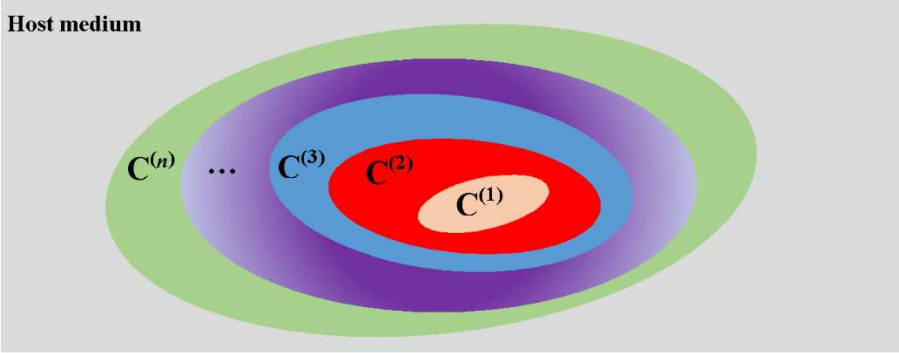

Figure 3. Schematic illustration of an n-phase ellipsoidal heterogeneity. Central inclusion is enclosed in n-1 ellipsoidal coatings that might take dissimilar orientations.

$$\underset{n}{\overline{\boldsymbol{\varepsilon}}} = \sum_{j=1}^{n} f_j \overline{\boldsymbol{\varepsilon}}^{(j)} \quad ; \qquad \underset{n}{\overline{\boldsymbol{\sigma}}} = \sum_{j=1}^{n} f_j \overline{\boldsymbol{\sigma}}^{(j)} = \sum_{j=1}^{n} f_j \mathbf{C}^{(j)} \overline{\boldsymbol{\varepsilon}}^{(j)} \tag{13}$$

The under-script *n* indicates that the related quantity is averaged over phases 1 to *n*. Using this form of representation, $\underset{n}{\overline{\boldsymbol{\varepsilon}}}$ and $\underset{n}{\overline{\boldsymbol{\sigma}}}$ are distinguished from the average of these quantities over the *n*th phase alone. Here, the relative volume fraction $f_j = V_j \Big/ \sum_{k=1}^{n} V_k$ is defined as the ratio of the volume of phase *j* to the volume of the entire heterogeneity. The equivalent stiffness of the *n*-phase heterogeneity, $\underset{n}{\mathbf{C}}^{\text{eq}}$, is simply defined as $\underset{n}{\overline{\boldsymbol{\sigma}}} = \underset{n}{\mathbf{C}}^{\text{eq}} \underset{n}{\overline{\boldsymbol{\varepsilon}}}$ which takes the following form by substitution from Eq.(13).

$$\underset{n}{\overline{\boldsymbol{\sigma}}} = \underset{n}{\mathbf{C}}^{\text{eq}} \underset{n}{\overline{\boldsymbol{\varepsilon}}} \qquad \text{or} \qquad \sum_{j=1}^{n} f_j \mathbf{C}^{(j)} \overline{\boldsymbol{\varepsilon}}^{(j)} = \underset{n}{\mathbf{C}}^{\text{eq}} \sum_{j=1}^{n} f_j \overline{\boldsymbol{\varepsilon}}^{(j)} \tag{14}$$

This last relationship can be decomposed as follows.

$$\sum_{j=1}^{n-1} f_j \mathbf{C}^{(j)} \overline{\boldsymbol{\varepsilon}}^{(j)} + f_n \mathbf{C}^{(n)} \overline{\boldsymbol{\varepsilon}}^{(n)} = \mathop{\mathbf{C}}_{n}^{\mathrm{eq}} \left[\sum_{j=1}^{n-1} f_j \overline{\boldsymbol{\varepsilon}}^{(j)} + f_n \overline{\boldsymbol{\varepsilon}}^{(n)} \right] \tag{15}$$

This decomposition helps to correlate $\mathop{\mathbf{C}}_{n}^{\mathrm{eq}}$ with $\mathop{\mathbf{C}}_{n-1}^{\mathrm{eq}}$, the equivalent stiffness of the sub-heterogeneity composed of phases 1 to *n*-1. For this sub-heterogeneity, the analogue of relationships (13) and (14) read

$$\begin{cases} \mathop{\overline{\boldsymbol{\varepsilon}}}_{n-1} = \sum_{j=1}^{n-1} \phi_j \overline{\boldsymbol{\varepsilon}}^{(j)} \\ \mathop{\overline{\boldsymbol{\sigma}}}_{n-1} = \sum_{j=1}^{n-1} \phi_j \overline{\boldsymbol{\sigma}}^{(j)} = \sum_{j=1}^{n-1} \phi_j \mathbf{C}^{(j)} \overline{\boldsymbol{\varepsilon}}^{(j)} \end{cases} ; \qquad \begin{cases} \mathop{\overline{\boldsymbol{\sigma}}}_{n-1} = \mathop{\mathbf{C}}_{n-1}^{\mathrm{eq}} \mathop{\overline{\boldsymbol{\varepsilon}}}_{n-1} \\ \sum_{j=1}^{n-1} \phi_j \mathbf{C}^{(j)} \overline{\boldsymbol{\varepsilon}}^{(j)} = \mathop{\mathbf{C}}_{n-1}^{\mathrm{eq}} \sum_{j=1}^{n-1} \phi_j \overline{\boldsymbol{\varepsilon}}^{(j)} \end{cases} \tag{16}$$

with the relative volume fraction ϕ_j defined as $\phi_j = V_j \Big/ \sum_{k=1}^{n-1} V_k$. One can easily show that ϕ_j and f_j are linearly correlated: $\phi_j = f_j / (1 - f_n)$. By using this equality, relationships (16) are rewritten as follows, in terms of initial volume fractions f_j instead of ϕ_j.

$$\begin{cases} \mathop{\overline{\boldsymbol{\varepsilon}}}_{n-1} = \dfrac{1}{1-f_n} \sum_{j=1}^{n-1} f_j \overline{\boldsymbol{\varepsilon}}^{(j)} \\ \mathop{\overline{\boldsymbol{\sigma}}}_{n-1} = \dfrac{1}{1-f_n} \sum_{j=1}^{n-1} f_j \mathbf{C}^{(j)} \overline{\boldsymbol{\varepsilon}}^{(j)} \end{cases} ; \quad \begin{cases} \mathop{\overline{\boldsymbol{\sigma}}}_{n-1} = \mathop{\mathbf{C}}_{n-1}^{\mathrm{eq}} \mathop{\overline{\boldsymbol{\varepsilon}}}_{n-1} \\ \sum_{j=1}^{n-1} f_j \mathbf{C}^{(j)} \overline{\boldsymbol{\varepsilon}}^{(j)} = \mathop{\mathbf{C}}_{n-1}^{\mathrm{eq}} \sum_{j=1}^{n-1} f_j \overline{\boldsymbol{\varepsilon}}^{(j)} \end{cases} \tag{17}$$

Simultaneous use of Eqs.(17) and (15) leads to the following equivalent relationships.

$$\begin{aligned} &\sum_{j=1}^{n-1} f_j \mathop{\mathbf{C}}_{n-1}^{\mathrm{eq}} \overline{\boldsymbol{\varepsilon}}^{(j)} + f_n \mathbf{C}^{(n)} \overline{\boldsymbol{\varepsilon}}^{(n)} = \mathop{\mathbf{C}}_{n}^{\mathrm{eq}} \left[\sum_{j=1}^{n-1} f_j \overline{\boldsymbol{\varepsilon}}^{(j)} + f_n \overline{\boldsymbol{\varepsilon}}^{(n)} \right] \\ \Rightarrow &\left(1-f_n\right) \mathop{\mathbf{C}}_{n-1}^{\mathrm{eq}} \mathop{\overline{\boldsymbol{\varepsilon}}}_{n-1} + f_n \mathbf{C}^{(n)} \overline{\boldsymbol{\varepsilon}}^{(n)} = \mathop{\mathbf{C}}_{n}^{\mathrm{eq}} \left[\left(1-f_n\right) \mathop{\overline{\boldsymbol{\varepsilon}}}_{n-1} + f_n \overline{\boldsymbol{\varepsilon}}^{(n)} \right] \end{aligned} \tag{18}$$

Definitions (18) are equivalent to the basic definition of $\mathop{\mathbf{C}}_{n}^{\mathrm{eq}}$ presented in (14) and can be used instead. The implication of the first equality in $(18)_1$ is that in the expression concerning the definition of $\mathop{\mathbf{C}}_{n}^{\mathrm{eq}}$, one can replace all $\mathbf{C}^{(j)}$, $j = 1,...,n-1$ with the homogeneous $\mathop{\mathbf{C}}_{n-1}^{\mathrm{eq}}$ without perturbing $\overline{\boldsymbol{\varepsilon}}^{(j)}$, and use this alternative expression for

defining $\mathbf{C}_n^{\text{eq}}$. The second equality in (18)$_2$ is similar to the first one except that the sum $\sum_{j=1}^{n-1} f_j \overline{\boldsymbol{\varepsilon}}^{(j)}$ is replaced with the corresponding equivalent term $\left(1-f_n\right)\overline{\boldsymbol{\varepsilon}}_{n-1}$ thus rendering the problem to a simple two-phase one. In case the equivalent stiffness $\mathbf{C}_{n-1}^{\text{eq}}$ is available or can be somehow identified, then within a two-phase heterogeneity setting in which $\mathbf{C}_{n-1}^{\text{eq}}$ is the stiffness of the core and $\mathbf{C}^{(n)}$ is the stiffness of the coating, Eq.(9) can be used to determine $\mathbf{C}_n^{\text{eq}}$. This is the key idea that connects $\mathbf{C}_n^{\text{eq}}$ to the exact Eq.(9). Rigorously speaking, instead of treating the *n*-phase heterogeneity in its original form, one may alternatively replace *n*-1 inner phases with one single phase characterized by $\mathbf{C}_{n-1}^{\text{eq}}$ and then in conjunction with $\mathbf{C}^{(n)}$ calculate $\mathbf{C}_n^{\text{eq}}$ using Eq.(9), no matter how the elastic fields are distributed.

A similar procedure can be followed to establish analogous relationships between $\mathbf{C}_{n-1}^{\text{eq}}$ and $\mathbf{C}_{n-2}^{\text{eq}}$, the equivalent stiffness of the sub-heterogeneity *n*-2 composed of phases 1 to *n*-2. The analogue of Eq.(18)$_2$ is then expressed as follows.

$$\left(1-\phi_{n-1}\right)\mathbf{C}_{n-2}^{\text{eq}}\,\overline{\boldsymbol{\varepsilon}}_{n-2}+\phi_{n-1}\mathbf{C}^{(n-1)}\overline{\boldsymbol{\varepsilon}}^{(n-1)}=\mathbf{C}_{n-1}^{\text{eq}}\left[\left(1-\phi_{n-1}\right)\overline{\boldsymbol{\varepsilon}}_{n-2}+\phi_{n-1}\overline{\boldsymbol{\varepsilon}}^{(n-1)}\right] \tag{19}$$

Note that the appropriate definition for relative volume fractions has to be used. Likewise, analogous relations can be written down for other sub-heterogeneities in a sequential manner until the deepest sub-heterogeneities are reached.

$$\begin{aligned}\left(1-\eta_3\right)\mathbf{C}_2^{\text{eq}}\,\overline{\boldsymbol{\varepsilon}}_2+\eta_3\mathbf{C}^{(3)}\overline{\boldsymbol{\varepsilon}}^{(3)}&=\mathbf{C}_3^{\text{eq}}\left[\left(1-\eta_3\right)\overline{\boldsymbol{\varepsilon}}_2+\eta_3\overline{\boldsymbol{\varepsilon}}^{(3)}\right]\\ \left(1-\nu_2\right)\mathbf{C}^{(1)}\overline{\boldsymbol{\varepsilon}}^{(1)}+\nu_2\mathbf{C}^{(2)}\overline{\boldsymbol{\varepsilon}}^{(2)}&=\mathbf{C}_2^{\text{eq}}\left[\left(1-\nu_2\right)\overline{\boldsymbol{\varepsilon}}^{(1)}+\nu_2\overline{\boldsymbol{\varepsilon}}^{(2)}\right]\end{aligned} \tag{20}$$

with $\eta_3=V_3/(V_1+V_2+V_3)$ and $\nu_2=V_2/(V_1+V_2)$. $\mathbf{C}_2^{\text{eq}}$ is calculated from Eq.(9) as the starting point. It is then plugged into Eq.(20)$_1$, a two-phase problem whose unknown is $\mathbf{C}_3^{\text{eq}}$ thus identifying $\mathbf{C}_3^{\text{eq}}$ by using Eq.(9) a second time. This recursive, layer-by-

layer sweeping procedure is then followed until the last layer is reached and $\mathbf{C}_n^{eq}$ is identified. In this manner, the equivalent stiffness calculation of an n-phase heterogeneity is broken down to n-1 two-phase problems. In other words, in a recursive sequence leading to the calculation of $\mathbf{C}_n^{eq}$, the starting point is $\mathbf{C}_2^{eq}$ and n-1 layers are swept in a layer-wise fashion within n-1 iterations.

Remarks:

- The above mathematical procedure concerning the elastic characterization of the equivalent inhomogeneity of any multiphase ellipsoidal heterogeneity by using the two-phase formula (9) is consistent with Hill's statement [33] explained in the last paragraph of §3 *op. cit*. In the context of calculating the overall elastic moduli of a generic "cylindrical composite element" made of two transversely isotropic phases, Hill asserts that for an n-phase composite cylinder, the overall moduli of the innermost two phases are first calculated using the two-phase equations. Both phases are then replaced with a single element characterized by the calculated overall moduli, which in combination with the next shell are viewed as a new two-phase composite cylinder and treated using the two-phase formulation. Likewise, the other shells are successively swept to update the equivalent inhomogeneity until the incorporation of the outermost shell.

- The above generalization of exact expression (9) from 2-phase to n-phase ellipsoidal compounds allows for the analysis of heterogeneities with radially graded interphases. In such cases where the elasticity of a layer varies continuously across the thickness (i.e. radially), one only has to subdivide the layer into sufficiently thin sublayers such that the elasticity of each sublayer is almost uniform. Then, using the above layer-wise sweeping procedure and without having to use any mathematical integration operation, the equivalent stiffness is readily obtained.

3. Results and discussion

To assess the performance of the equivalent inhomogeneity estimators discussed hereinabove, several numerical examples of two- and three-phase spherical heterogeneities as well as two examples of three-phase spheroidal heterogeneities with different stiffness ratios are examined in this section. For two-level homogenization part, GEEE is separately used in combination with FEM and MT techniques. Comparison is particularly made with (n+1)-phase model and ACI model, two relevant non Eshelby-type approaches. The assumption of perfect bonding between the adjacent components prevails in all examples. For verification purposes, H-S bounds of the equivalent bulk and shear moduli of the spherical configurations are also calculated. The H-S bounds relations for multiphase spheres are given in Appendix C. In the following, "reference values" signifies the results of GEEE and modified HNNM, as their outputs are always identical.

3.1. Two-phase spherical heterogeneities

In the following numerical examples, the Poisson's ratio of all phases is fixed at 0.3, unless otherwise specified, while their Young's moduli are let vary to create stiffness contrasts. Two numerical examples of two-phase core/shell spheres along with their effective stiffnesses evaluated using different estimators are summarized in Table 1. The core/shell stiffness ratios in both examples are 10^{-2} and 10^{2}. As reflected in Table 1, the results of GEEE and modified HNNM match perfectly. Such a perfect agreement is also seen in other spherical examples given further below.

Regarding the performance of HNNM, it can be seen that for neither of equivalent moduli of the two-phase examples of Table 1, HNNM gives satisfactory results. This estimator exhibits a similar performance in other numerical examples too (see Table 2, 3, 4 and Figure 4). Nonetheless, HNNM results always fulfil the respective H-S bounds. Naturally, the deviation of equivalent moduli returned by HNNM from the reference values is attenuated by lowering the contrast between the

elastic moduli of constituting phases. This feature is illustrated and discussed further in the following subsection. It is underlined that in all numerical examples and for the solution of implicit equations of HNNM and modified HNNM, we ensured that the results are not influenced by the numerical techniques employed.

Table 1. Equivalent moduli of two spherical core/shell examples as identified by different estimators. In both examples, Poisson's ratio of the constituting phases is 0.3. In the 1st example, the core is two orders of magnitude more compliant than the shell and vice versa in the 2nd example.

	1st ex.: $E_{core}/E_{shell}=10^{-2}$		2nd ex.: $E_{core}/E_{shell}=10^{2}$		Remarks
	K (GPa)	μ (GPa)	K (GPa)	μ (GPa)	
Core	8.33×10^{-1}	3.85×10^{-1}	8.33×10^{1}	3.85×10^{1}	Diameter = 100 nm
Shell	8.33×10^{1}	3.85×10^{1}	8.33×10^{-1}	3.85×10^{-1}	Outer diameter = 120 nm
GEEE	18.97	10.97	2.61	1.44	-
HNNM	3.20	1.99	12.97	8.26	* In disagreement with GEEE
modified HNNM	18.97	10.97	2.61	1.44	In agreement with GEEE
H-S lower bounds	1.79	0.95	2.61	1.44	-
H-S upper bounds	18.97	10.97	29.47	16.40	-

* Unless the contrast between core/shell moduli is low, the estimated equivalent moduli by HNNM are nowhere close to exact values, hence this estimator is inaccurate and unsatisfactory in general (cf. **Figure 4**).

3.2. Three-phase spherical and spheroidal heterogeneities

Evaluating the performance of the aforementioned estimators in determining the equivalent moduli of three-phase spherical and spheroidal heterogeneities is undertaken in this subsection. In the numerical examples of spherical heterogeneities, the Poisson's ratio of the constituents is fixed at 0.3, while their Young's moduli are let vary. In the third numerical example of Table 2, the inner core is more compliant than the intermediate shell, which is in turn more compliant than the outer shell. In the fourth numerical example, the inner core is stiffer than the intermediate shell, which is stiffer than the outer shell. In both examples, the ratio of elastic moduli between two adjacent constituents is 10^{1}. Similar to two-phase numerical examples of Table 1, GEEE and modified HNNM are always in perfect agreement, regardless of the contrast between the phases' moduli. Regarding the performance of HNNM estimator, similar to the previous examples, neither of the

equivalent elastic moduli agree with the corresponding reference values. Nonetheless, they lie inside their respective H-S bounds.

Table 2. Similar to Table 1 but for a three-phase spherical heterogeneity. In both examples, the phases' Poisson's ratio is fixed at 0.3 while the Young's moduli differ one order of magnitude from their adjacent phase. In the 3rd example, the core is the most compliant phase and vice versa in the 4th example.

	3rd ex.: $E_{core}/E_{shell(1)} = 10^{-1}$, $E_{shell(1)}/E_{shell(2)} = 10^{-1}$		4th ex.: $E_{core}/E_{shell(1)} = 10^{+1}$, $E_{shell(1)}/E_{shell(2)} = 10^{+1}$		Remarks
	K (GPa)	μ (GPa)	K (GPa)	μ (GPa)	
Core	8.33×10^{-1}	3.85×10^{-1}	8.33×10^{1}	3.85×10^{1}	Diameter = 100 nm
Shell (1)	8.33	3.85	8.33	3.85	outer diameter = 120 nm
Shell (2)	8.33×10^{1}	3.85×10^{1}	8.33×10^{-1}	3.85×10^{-1}	outer diameter = 140 nm
GEEE	18.04	10.35	2.78	1.52	-
HNNM	6.84	4.09	6.59	3.94	* In disagreement with GEEE
modified HNNM	18.04	10.35	2.78	1.52	In agreement with GEEE
H-S lower bounds	2.76	1.49	2.72	1.46	-
H-S upper bounds	19.17	10.69	18.83	10.51	-

* : See footnote of Table 1.

To probe deeper into our analysis, the numerical examples of Table 3 and 4 are presented, which concern a composite heterogeneity made of three homothetic, concentric spheroids. The similar diameters of the spheroids correspond those of the examples of Table 2. The aspect ratio of the spheroids, defined as the ratio of dissimilar axis to similar ones, is chosen 5. The state of the Young's moduli of the example of Table 3 and that of Table 4 is identical with, respectively, the 3rd and 4th example of Table 2. For performance evaluation purposes, the Poisson's ratios of the phases are chosen different than 0.3. The hypothetical Poisson's ratios 0.05, 0.2 and 0.45 are respectively assigned to the core, the first and second coating. To calculate Eshelby's tensors, we used the analytical relationships derived by Withers et al. [34] for spheroidal geometries with reference media no weaker than transverse isotropy such that the dissimilar axis of the spheroid, *viz.* z- or 3-axis, is normal to the plane of isotropy. Note that the final symmetry of the equivalent stiffnesses is transverse isotropy. As a common practice, instead of working with C_{11} and C_{12}, we opt for K_{12} and μ_{12}, the plane bulk and shear moduli, as two out of five independent elastic

constants of equivalent stiffnesses. It can be seen that again modified HNNM returns the same results that GEEE does and HNNM shows deviation from reference values.

Table 3. Similar to 3rd example of Table 2 but for concentric, homothetic spheroids with aspect ratio 5. Hypothetical Poisson's ratios of core, shell(1) and shell(2) are respectively, 0.05, 0.2 and 0.45.

	5th ex.: $E_{core}/E_{shell(1)} = 10^{-1}$, $E_{shell(1)}/E_{shell(2)} = 10^{-1}$					**Remarks**
	C_{13} **(GPa)**	C_{33} **(GPa)**	C_{44} **(GPa)**	$K_{12} = (C_{11}+C_{12})/2$ **(GPa)**	$\mu_{12} = C_{66} = (C_{11}-C_{12})/2$ **(GPa)**	
Core	0.053	1.01	0.48	0.53	0.48	similar diameters = 100 nm
Shell (1)	2.78	11.11	4.17	6.94	4.17	outer similar diameters = 120 nm
Shell (2)	310.34	379.31	34.48	344.83	34.48	outer similar diameters = 140 nm
GEEE	17.90	52.55	9.75	21.54	8.72	-
HNNM	3.13	31.47	4.76	4.54	2.61	* In disagreement with GEEE
modified HNNM	17.90	52.55	9.75	21.54	8.72	In agreement with GEEE

Table 4. Similar to 4th example of Table 2 but for concentric, homothetic spheroids with aspect ratio 5. Hypothetical Poisson's ratios of core, shell(1) and shell(2) are respectively, 0.05, 0.2 and 0.45.

	6th ex.: $E_{core}/E_{shell(1)} = 10^{+1}$, $E_{shell(1)}/E_{shell(2)} = 10^{+1}$					**Remarks**
	C_{13} **(GPa)**	C_{33} **(GPa)**	C_{44} **(GPa)**	$K_{12} = (C_{11}+C_{12})/2$ **(GPa)**	$\mu_{12} = C_{66} = (C_{11}-C_{12})/2$ **(GPa)**	
Core	5.29	100.53	47.62	52.91	47.62	similar diameters = 100 nm
Shell (1)	2.78	11.11	4.17	6.94	4.17	outer similar diameters = 120 nm
Shell (2)	3.10	3.79	0.34	3.45	0.34	outer similar diameters = 140 nm
GEEE	5.24	14.70	1.44	6.93	1.29	-
HNNM	4.12	30.73	4.80	7.96	2.74	* In disagreement with GEEE
modified HNNM	5.24	14.70	1.44	6.93	1.29	In agreement with GEEE

To complete our appraisal of the performance of the above estimators, the normalized equivalent moduli of a three-phase spherical heterogeneity taking a wide range of stiffness ratios are plotted in Figure 4. We opted for constant radii and Poisson's ratios, similar to the numerical examples of Table 2. Unlike the example of

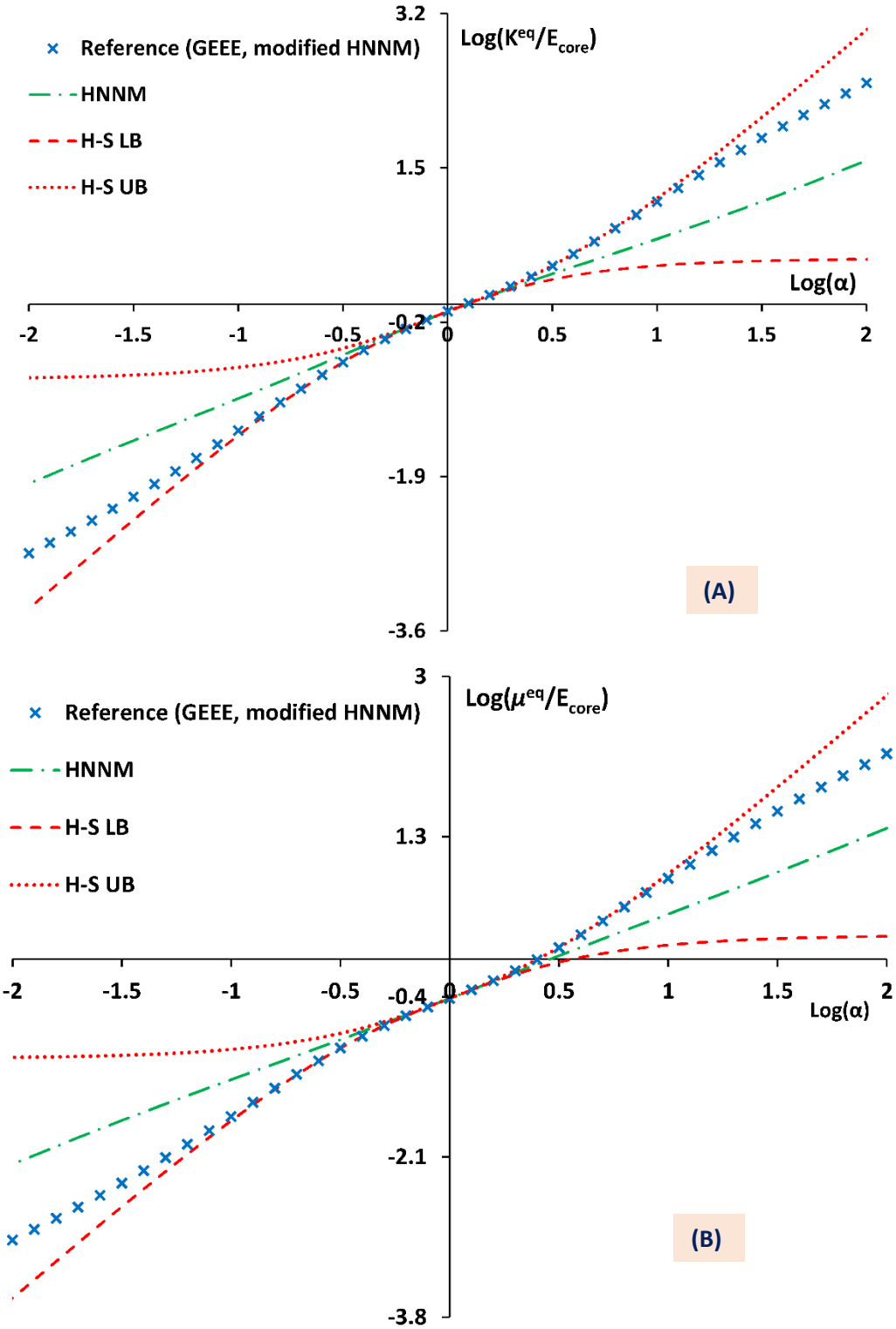

Figure 4 Log-Log plots of normalized ***(A)*** K^{eq} *and* ***(B)*** μ^{eq} *returned by different estimators for a three-phase spherical configuration. The geometry of the heterogeneity is identical with the examples of Table 2 and remains unchanged. The abscissa of both figures is the ratio of the Young's moduli of the phases defined as* $\alpha = E_{core}/E_{shell(2)} = E_{shell(2)}/E_{shell(1)}$. *In general, the less successful estimator is HNNM.*

Table 2, the modulus ratio between the phases, $\alpha = E_{\text{core}}/E_{\text{shell(2)}} = E_{\text{shell(2)}}/E_{\text{shell(1)}}$, is defined such that the monotony of the elasticity contrast between the phases from the core to the outer shell is perturbed. This helps to study the relative position of the

equivalent elastic moduli and their corresponding H-S bounds. α ratio is let vary continuously from 10^{-2} to 10^{+2} and then the equivalent bulk and shear moduli are estimated using the above estimators.

Figure 4 confirms that modified HNNM and GEEE results coincide over the entire range of elasticity contrast, in agreement with the results of Table 1-4, . In two forthcoming papers discussing cylindrical and platelet compounds, a similar agreement between these two estimators is demonstrated. The intuitive explanation for this observation lies most likely in the idea of "multiple reference media" that was introduced by Aboutajeddine and Neale [35] for the double-inclusion problem, and employed later on by Dinzart et al. [16] for the multi-inclusion problem. Likewise, in GEEE, after each intermediate equivalent stiffness calculation, the reference medium for calculating the polarization/Eshelby tensors is updated. This characteristic feature is common between both estimators and helps to have a better understanding of the complete agreement between GEEE and modified HNNM for a wide range of numerical examples we tested. Unlike GEEE, modified HNNM has a system of coupled, nonlinear, tensor equations. This is a major drawback of modified HNNM which significantly limits its practical applications.

In relation to the performance of HNNM estimator, similar to Table 1-4, it fails to match reference values. Nonetheless, the calculated moduli always meet the respective H-S bounds. A similar performance is exhibited by HNNM in treating composite cylinders, as will be discussed in a follow-up study. However, for weak contrasts between the stiffnesses, say $-0.5 < \mathrm{Log}(\alpha) < 0.5$, HNNM results are in good agreement with reference values.

In the examples of Table 1 and Table 2, there is a clear agreement between the reference equivalent moduli and one of their corresponding H-S bounds. Such an agreement, however, does no longer exist in the example of Figure 4. Examination of a large number of numerical examples of multiphase spherical compounds (including those not given here) have led us to the following conjecture regarding the state of

reference equivalent moduli with respect to their corresponding H-S bounds: *when the contrast between the bulk and shear moduli of the phases changes monotonically (decreasing or increasing) from the core to the outmost shell, the reference equivalent moduli agree with either of H-S bounds*. For two-phase compounds, the bulk and shear moduli of one of phases is always greater than its counterpart in the other phase, except for the trivial case of identical moduli. For this class of heterogeneities, a complete agreement between the reference moduli and one of the H-S bounds always exists. For other multiphase spherical particles, when the bulk and shear moduli change radially monotonically, the reference equivalent moduli continue to be fairly close to one of the H-S bounds. Numerical examples of Table 2 belong to this class of core-shell heterogeneities. However, if the monotonic change in stiffness from the core to the outmost layer is perturbed, as is the case of the numerical example of Figure 4, except for rather weak contrasts, the reference moduli are no more close to H-S bounds (Note the Log-Log scale of the plots). The mathematical proof of this conclusion being beyond our capability, we call it a conjecture.

3.3. Comparison with (n+1)-phase model and ACI model

To assess the validity of our proposed estimator, we compare it with two relevant non Eshelby-type models that are specifically developed for studying multiphase spherical heterogeneities. These two estimators are (n+1)-phase model [18] and Annular Coated Inclusion (ACI) model [20].

In the comparison made with (n+1)-phase model, the effective elastic moduli of a three-phase composite made of a host matrix containing two-phase spherical inclusions arranged in a cubic array of infinite extent are numerically evaluated using finite element method for several volume fractions. From among different possible combinations of elasticity contrasts between the phases, we choose a case where the coating is stiffer than the matrix, which is in turn stiffer than the core.

$E_{\text{coating}} = 100\,\text{GPa}$, $E_{\text{m}} = 80\,\text{GPa}$ and $E_{\text{core}} = 1\,\text{GPa}$ are Young's moduli chosen for the phases and their Poisson's ratio is 0.3. Three types of analyses have been carried out:

- Type A) where each phase is modeled using its proper dimensions, meshed and FE analyzed; the outputs of this Type are considered as reference values.
- Type B) where the core-shell compound is replaced with the equivalent inhomogeneity determined from (n+1)-phase model, before meshing and FE analysis.
- Type C) where the core-shell compound is replaced with the equivalent inhomogeneity determined from our developed GEEE, before meshing and FE analysis.

For different volume fractions, the corresponding numerical results of each type of analysis are tabulated in Table 5. It can be immediately seen that both Types of two-level homogenization of B, C give very close results to corresponding reference values, namely Type A, with a slight advantage in favor of Type C results, which is based on GEEE, since Dev_B < Dev_C.

Table 5. Comparison of hybrid analyses of GEEE/FE and (n+1)-phase/FE with reference FE results for three-phase composites filled with coated spherical inclusions arranged in cubic arrays. In each case, core and coating share the same volume fraction.

Effective moduli	**Type A**	**Type B**	**Type C**	**Dev_B** =100× |**A-B**|/**A**	**Dev_C** =100× |**A-C**|/**A**	f_{eq}
C_{11} (GPa)	98.19	97.83	98.16	0.37	0.031	
C_{12} (GPa)	40.98	41.113	40.94	0.33	0.10	f_{eq} = 0.1
C_{66} (GPa)	28.46	28.213	28.495	0.89	0.11	
C_{11} (GPa)	89.92	89.15	89.74	0.86	0.20	
C_{12} (GPa)	36.392	36.67	36.36	0.77	0.09	f_{eq} = 0.2
C_{66} (GPa)	26.302	25.81	26.35	1.83	0.2	
C_{11} (GPa)	82.54	81.23	82.05	1.59	0.59	
C_{12} (GPa)	32.30	32.75	32.32	1.4	0.06	f_{eq} = 0.3
C_{66} (GPa)	24.24	23.56	24.32	2.78	0.34	
C_{11} (GPa)	75.92	73.90	74.96	2.66	1.27	
C_{12} (GPa)	28.67	29.30	28.77	2.22	0.35	f_{eq} = 0.4
C_{66} (GPa)	22.28	21.47	22.43	3.63	0.65	
C_{11} (GPa)	69.76	66.78	68.09	4.26	2.40	
C_{12} (GPa)	25.35	26.16	25.53	3.19	0.71	f_{eq} = 0.5
C_{66} (GPa)	20.36	19.49	20.62	4.28	1.27	

The FEM calculations were performed using ABAQUS software. As illustrated in Figure 5, the representative unit cell (RUC) of the cubic array was discretized with 10-node tetrahedral solid quadratic elements, whose characteristic size was 2% of the RUC edge length. We took advantage of the symmetric features of the RUC to model 1/8 of it and ended up with 94529 elements (133780 nodes). In the reference model associated with Type A analyses illustrated in Figure 5a, the coating is discretized with four rows of elements. In two other FE models associated with two-level homogenization of Type B, C, the distribution of elastic fields are qualitatively similar in agreement with the quantitative results of Table 5. Knowing that the elastic fields in none of the phases are uniform, contour plots of stress field clearly show that this nonuniformity is more pronounced in the equivalent inhomogeneity than in the core phase of the reference model.

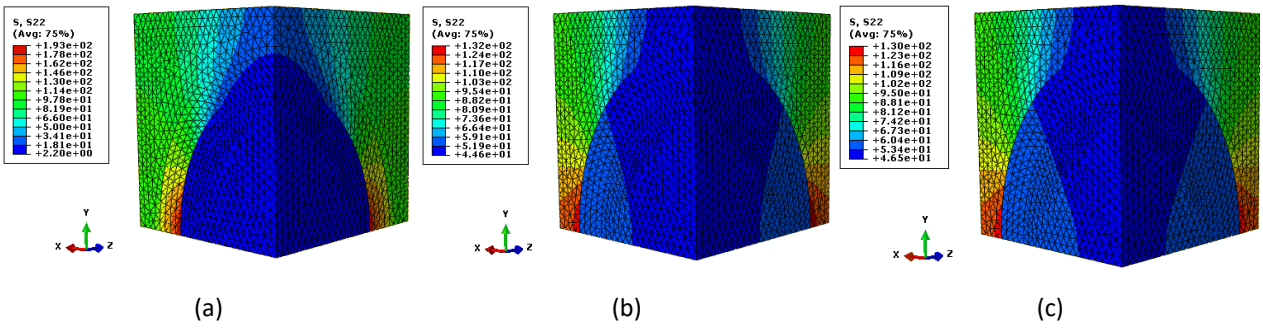

Figure 5. Contour plots of the stress distribution inside 1/8 of the RUCs associated with FE analyses of Table 5 for f_{eq}=0.3.

In the comparison made with ACI model, which is a relevant model developed in [20] for isotropic composites reinforced with spherical core-shell inclusions, a two-level homogenization of GEEE/MT is carried out. What distinguishes ACI model is the way the localization tensor of fillers is calculated by accounting for the presence of coating around each inclusion immersed in the binding matrix. According to the authors of ACI, there is a need for such a model as the commonly used Mori-Tanaka (MT) method with the approximated Eshelby-based localization tensor does not yield satisfactory results, especially for soft coatings. The numerical examples of

Fig.4b in [20] are re-examined here. As illustrated in Figure 5, the two-level scheme of GEEE/MT yields satisfactorily close enough results to accurate ACI values, in both cases of relative core-shell volume fractions considered, whereas the error of direct MT analysis turns out to be far larger. Note that ACI is an estimator that is specifically developed for this configuration and is presented to be more accurate than MT method for associated composite systems, as claimed by its authors. The implementation of ACI however is not as simple as the hybrid GEEE/MT. With its complementary analogue developed for three-phase composites reinforced with long cylindrical coated fillers, ACI is confined to these two configurations. Additionally, although its implementation is relatively simpler for spherical inclusions, it is much more complicated for the cylindrical fillers. On the other hand, the results of GEEE/MT can be used insightfully as it gives acceptable predictions compared to approaches such as direct MT, especially when we consider the simplicity and versatility of GEEE, which outweighs the small error that its assumptions impart into the effective properties calculation.

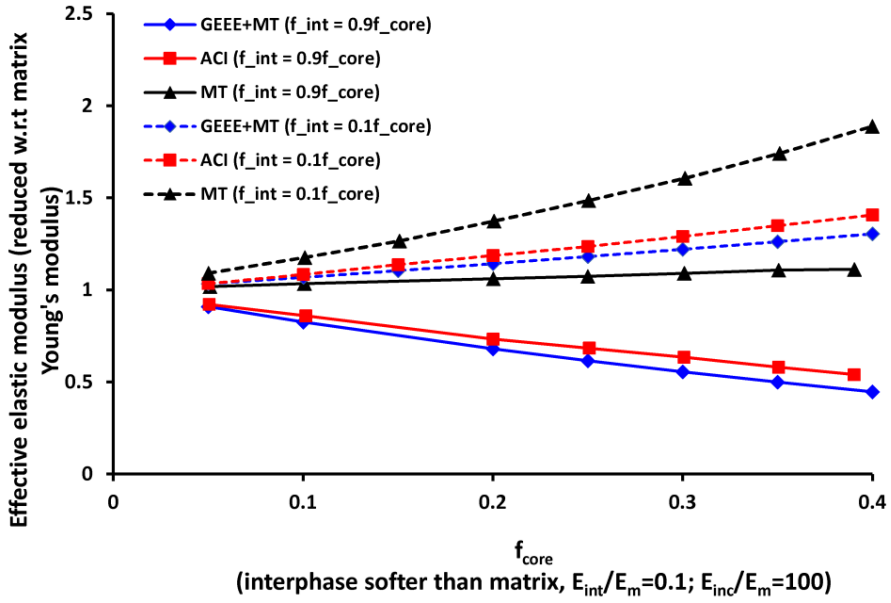

Figure 6. Normalized effective elastic modulus of a three-phase isotropic composite containing spherical coated inclusions. The numerical example of Fig.4b in [20] *is re-examined using ACI model op. cit. and the two-level GEEE/MT.*

4. Summary and conclusion

An efficient, general and explicit Eshelby-type estimator, called GEEE, for the equivalent stiffness calculation of multiphase ellipsoidal heterogeneities has been developed and evaluated. The popular configuration of spherical and spheroidal heterogeneities made of isotropic phases has been chosen for numerical analysis and performance evaluation purposes. To this end, two other Eshelby-type estimators, namely HNNM and modified HNNM, together with the Hashin-Shtrikman bounds have also been implemented. Examination of several numerical examples and related plots of equivalent elastic moduli over a wide range of stiffness ratios of multiphase spherical heterogeneities revealed that:

- GEEE, as an Eshelby-type estimator like modified HNNM, is flexible enough to be applied to a wide range of geometries. Unlike modified HNNM, GEEE consists of an explicit and linear tensor equation that is recursively run. Implementation of this estimator requires elementary matrix operations together with the appropriate form of Eshelby's tensor.
- The less successful estimator turns out to be HNNM. Implementation of this estimator requires numerical techniques for finding the roots of the associated nonlinear tensor equation (cf. Appendix A). Unless the contrast between the constituents' stiffnesses is low, a huge difference between the results of HNNM estimator and the corresponding reference values is observed.
- Generalization of GEEE to multiphase ellipsoidal heterogeneities leads to a direct framework for the characterization of heterogeneities in which the elasticity of one or more coating(s) is radially graded. In this event, one needs to subdivide the inhomogeneous coating(s) into subshells such that the elastic properties are nearly uniform across each subshell. Next, an appropriate estimator such as GEEE is used for finding the equivalent elasticity of the entire heterogeneity by starting from the innermost phases and sweeping each

layer/subshell. This analysis may be redone with a finer subdivision of the radially graded coating(s) to ensure the adequate accuracy of the estimated equivalent elastic moduli.

- Breaking the homogenization problem into two or multiple levels usually requires simplifying assumptions, which normally adds some error into the results. With regard to hybrid analyses of GEEE/FE and GEEE/MT, the performance of the proposed estimator has been quite satisfactory and the deviation from the reference values has been sufficiently small.

Funding

ANR (*Agence Nationale de la Recherche*) and CGI (*Commissariat à l'Investissement d'Avenir*) are gratefully acknowledged for their financial support through Labex SEAM (Science and Engineering for Advanced Materials and devices), ANR 11 LABX 086, ANR 11 IDEX 05 02.

Competing interests

Authors have no competing interests to declare.

References

1. Mogilevskaya SG, Stolarski HK, Crouch SL. 2012 On Maxwell's concept of equivalent inhomogeneity: When do the interactions matter? *J. Mech. Phys. Solids* **60**, 391–417. (doi:10.1016/j.jmps.2011.12.008)

2. Zhu XY, Wang X, Yu Y. 2014 Micromechanical creep models for asphalt-based multi-phase particle-reinforced composites with viscoelastic imperfect interface. *Int. J. Eng. Sci.* **76**, 34–46. (doi:10.1016/j.ijengsci.2013.11.011)

3. Tran B V., Pham DC, Nguyen THG. 2015 Equivalent-inclusion approach and effective medium approximations for elastic moduli of compound-inclusion composites. *Arch. Appl. Mech.* **85**, 1983–1995. (doi:10.1007/s00419-015-1031-6)

4. Nazarenko L, Stolarski H. 2016 Energy-based definition of equivalent inhomogeneity for various interphase models and analysis of effective properties of particulate composites. *Compos. Part B Eng.* **94**, 82–94. (doi:10.1016/j.compositesb.2016.03.015)

5. Jiang Z, Xi Y, Gu X, Huang Q, Zhang W. 2016 Mesoscopic Predictions of Cement Mortar Diffusivity by Analytical and Numerical Methods. *J. Mater. Civ. Eng.* , 04016256. (doi:10.1061/(ASCE)MT.1943-5533.0001805)

6. Kushch VI, Sevostianov I. 2016 Maxwell homogenization scheme as a rigorous method of micromechanics: Application to effective conductivity of a composite with spheroidal particles. *Int. J. Eng. Sci.* **98**, 36–50. (doi:10.1016/j.ijengsci.2015.07.003)

7. Giordano S. 2016 Nonlinear effective behavior of a dispersion of randomly oriented coated ellipsoids with arbitrary temporal dispersion. *Int. J. Eng. Sci.* **98**, 14–35. (doi:10.1016/j.ijengsci.2015.07.009)

8. Shen L, Li J. 2005 Homogenization of a fibre/sphere with an inhomogeneous interphase for the effective elastic moduli of composites. *Proc. R. Soc. A Math. Phys. Eng. Sci.* **461**, 1475–1504. (doi:10.1098/rspa.2005.1447)

9. Chatzigeorgiou G, Seidel GD, Lagoudas DC. 2012 Effective mechanical properties of "fuzzy fiber" composites. *Compos. Part B Eng.* **43**, 2577–2593. (doi:10.1016/j.compositesb.2012.03.001)

10. Duan HL, Yi X, Huang ZP, Wang J. 2007 A unified scheme for prediction of effective moduli of multiphase composites with interface effects: Part II—Application and scaling laws. *Mech. Mater.* **39**, 94–103. (doi:10.1016/j.mechmat.2006.02.010)

11. Friebel C, Doghri I, Legat V. 2006 General mean-field homogenization schemes for viscoelastic composites containing multiple phases of coated inclusions. *Int. J. Solids Struct.* **43**, 2513–2541. (doi:10.1016/j.ijsolstr.2005.06.035)

12. Nemat-Nasser S, Hori M. 1999 *Micromechanics: overall properties of heterogeneous materials*. Elsevier.

13. Torquato S. 2002 *Random Heterogeneous Materials*. New York, NY: Springer New York. (doi:10.1007/978-1-4757-6355-3)

14. Eshelby JD. 1957 The determination of the elastic field of an ellipsoidal inclusion, and related problems. *Proc. R. Soc. London. Ser. A. Math. Phys. Sci.* **241**, 376–396. (doi:10.1098/rspa.1957.0133)

15. Hori M, Nemat-Nasser S. 1993 Double-inclusion model and overall moduli of multi-phase composites. *Mech. Mater.* **14**, 189–206. (doi:10.1016/0167-6636(93)90066-Z)

16. Dinzart F, Sabar H, Berbenni S. 2016 Homogenization of multi-phase composites based on a revisited formulation of the multi-coated inclusion problem. *Int. J. Eng. Sci.* **100**, 136–151. (doi:10.1016/j.ijengsci.2015.12.001)

17. Hashin Z. 1962 The Elastic Moduli of Heterogeneous Materials. *J. Appl. Mech.* **29**, 143. (doi:10.1115/1.3636446)

18. Hervé E, Zaoui A. 1993 inclusion-based micromechanical modelling. *Int. J. Eng. Sci.* **31**, 1–10. (doi:10.1016/0020-7225(93)90059-4)

19. McCartney LN, Kelly A. 2008 Maxwell's far-field methodology applied to the prediction of properties of multi-phase isotropic particulate composites. *Proc. R. Soc. A Math. Phys. Eng. Sci.* **464**, 423–446. (doi:10.1098/rspa.2007.0071)

20. Wang Z, Oelkers RJ, Lee KC, Fisher FT. 2016 Annular Coated Inclusion model and applications for polymer nanocomposites – Part I: Spherical inclusions. *Mech. Mater.* **101**, 170–184. (doi:10.1016/J.MECHMAT.2016.07.004)

21. Li G, Zhao Y, Pang S-S, Li Y. 1999 Effective Young's modulus estimation of concrete. *Cem. Concr. Res.* **29**, 1455–1462. (doi:10.1016/S0008-8846(99)00119-2)

22. Odegard GM, Clancy TC, Gates TS. 2005 Modeling of the mechanical properties of nanoparticle/polymer composites. *Polymer (Guildf).* **46**, 553–562. (doi:10.1016/j.polymer.2004.11.022)

23. Duan HL, Jiao Y, Yi X, Huang ZP, Wang J. 2006 Solutions of inhomogeneity problems with graded shells and application to core–shell nanoparticles and composites. *J. Mech. Phys. Solids* **54**, 1401–1425. (doi:10.1016/j.jmps.2006.01.005)

24. Diani J, Gilormini P, Merckel Y, Vion-Loisel F. 2013 Micromechanical modeling of the linear viscoelasticity of carbon-black filled styrene butadiene rubbers: The role of the filler–rubber interphase. *Mech. Mater.* **59**, 65–72. (doi:10.1016/j.mechmat.2012.12.007)

25. Bardella L, Genna F. 2001 On the elastic behavior of syntactic foams. *Int. J.*

Solids Struct. **38**, 7235–7260. (doi:10.1016/S0020-7683(00)00228-6)

26. Bardella L, Sfreddo A, Ventura C, Porfiri M, Gupta N. 2012 A critical evaluation of micromechanical models for syntactic foams. *Mech. Mater.* **50**, 53–69. (doi:10.1016/j.mechmat.2012.02.008)

27. Zheng J, Zhou X, Jin X. 2012 An n-layered spherical inclusion model for predicting the elastic moduli of concrete with inhomogeneous ITZ. *Cem. Concr. Compos.* **34**, 716–723. (doi:10.1016/j.cemconcomp.2012.01.011)

28. Anisimova M, Knyazeva A, Sevostianov I. 2016 Effective thermal properties of an aluminum matrix composite with coated diamond inhomogeneities. *Int. J. Eng. Sci.* **106**, 142–154. (doi:10.1016/j.ijengsci.2016.05.010)

29. Young BA, Fujii AMK, Thiele AM, Kumar A, Sant G, Taciroglu E, Pilon L. 2016 Effective elastic moduli of core-shell-matrix composites. *Mech. Mater.* **92**, 94–106. (doi:10.1016/j.mechmat.2015.09.006)

30. Eshelby JD. 1961 Elastic inclusions and inhomogeneities. *Prog. solid Mech.* **2**, 89–140.

31. Ponte Castañeda P, Willis JR. 1995 The effect of spatial distribution on the effective behavior of composite materials and cracked media. *J. Mech. Phys. Solids* **43**, 1919–1951. (doi:10.1016/0022-5096(95)00058-Q)

32. Willis JR. 1977 Bounds and self-consistent estimates for the overall properties of anisotropic composites. *J. Mech. Phys. Solids* **25**, 185–202. (doi:10.1016/0022-5096(77)90022-9)

33. Hill R. 1964 Theory of mechanical properties of fibre-strengthened materials: I. Elastic behaviour. *J. Mech. Phys. Solids* **12**, 199–212. (doi:10.1016/0022-5096(64)90019-5)

34. Withers P. 1989 The determination of the elastic field of an ellipsoidal inclusion in a transversely isotropic medium, and its relevance to composite materials. *Philos. Mag. A* **59**, 759–781. (doi:10.1080/01418618908209819)

35. Aboutajeddine A, Neale KW. 2005 The double-inclusion model: a new formulation and new estimates. *Mech. Mater.* **37**, 331–341. (doi:10.1016/j.mechmat.2003.08.016)

36. Parnell WJ, Calvo-Jurado C. 2015 On the computation of the Hashin–Shtrikman bounds for transversely isotropic two-phase linear elastic fibre-reinforced composites. *J. Eng. Math.* **95**, 295–323. (doi:10.1007/s10665-014-9777-3)

37. Parnell WJ. 2016 The Eshelby, Hill, Moment and Concentration Tensors for Ellipsoidal Inhomogeneities in the Newtonian Potential Problem and Linear Elastostatics. *J. Elast.* **125**, 231–294. (doi:10.1007/s10659-016-9573-6)

38. Hashin Z, Shtrikman S. 1963 A variational approach to the theory of the elastic behaviour of multiphase materials. *J. Mech. Phys. Solids* **11**, 127–140. (doi:10.1016/0022-5096(63)90060-7)

Appendix A

In the same work that Hori and Nemat-Nasser [15] proposed the well-known Double-Inclusion Model, they presented its generalization to multilayer ellipsoidal inclusions by following a similar procedure. Relations (5.1) to (5.5) in [15] are exploited here to find the adapted HNNM formulation to very long, multiphase cylinders. The consistency conditions for a multilayer inclusion composed of N phases are expressed as follows.

$$\begin{cases} \mathbf{C}\left(\boldsymbol{\varepsilon}^{\infty}+\left\langle\boldsymbol{\varepsilon}^{\mathrm{p}}\right\rangle_{\Omega_1}-\left\langle\boldsymbol{\varepsilon}^{*}\right\rangle_{\Omega_1}\right)=\mathbf{C}^{(1)}\left(\boldsymbol{\varepsilon}^{\infty}+\left\langle\boldsymbol{\varepsilon}^{\mathrm{p}}\right\rangle_{\Omega_1}\right) \\ \mathbf{C}\left(\boldsymbol{\varepsilon}^{\infty}+\left\langle\boldsymbol{\varepsilon}^{\mathrm{p}}\right\rangle_{\Gamma_2}-\left\langle\boldsymbol{\varepsilon}^{*}\right\rangle_{\Gamma_2}\right)=\mathbf{C}^{(2)}\left(\boldsymbol{\varepsilon}^{\infty}+\left\langle\boldsymbol{\varepsilon}^{\mathrm{p}}\right\rangle_{\Gamma_2}\right) \\ \vdots \\ \mathbf{C}\left(\boldsymbol{\varepsilon}^{\infty}+\left\langle\boldsymbol{\varepsilon}^{\mathrm{p}}\right\rangle_{\Gamma_N}-\left\langle\boldsymbol{\varepsilon}^{*}\right\rangle_{\Gamma_N}\right)=\mathbf{C}^{(N)}\left(\boldsymbol{\varepsilon}^{\infty}+\left\langle\boldsymbol{\varepsilon}^{\mathrm{p}}\right\rangle_{\Gamma_N}\right) \end{cases} \tag{A.1}$$

For convenience, the same symbols and notations employed in [15] are used here. To recapitulate, the elasticity of the reference medium and that of phase 'i' are denoted by $\mathbf{C}$ and $\mathbf{C}^{(i)}$, respectively; Ω_1 and Γ_i represent the region of space occupied by the innermost inclusion and phase 'i', respectively; $\left\langle\boldsymbol{\varepsilon}^{*}\right\rangle_{\Omega_1/\Gamma_i}$ and $\left\langle\boldsymbol{\varepsilon}^{\mathrm{p}}\right\rangle_{\Omega_1/\Gamma_i}$ are, respectively, the average transformation strain over Ω_1/Γ_i and the average perturbation strain over Ω_1/Γ_i. Remember that the angle brackets $\langle\ \rangle$ used in [15] has the same function as the overbar sign '$\bar{\ }$' we used in §2.2. Finally, $\boldsymbol{\varepsilon}^{\infty}$ stands for the far field strain. Rearranging the system of equations (A.1) yields

$$\begin{cases} \left(\mathbf{C}-\mathbf{C}^{(1)}\right)^{-1}\mathbf{C}\left\langle\boldsymbol{\varepsilon}^{*}\right\rangle_{\Omega_1}-\left\langle\boldsymbol{\varepsilon}^{\mathrm{p}}\right\rangle_{\Omega_1}=\boldsymbol{\varepsilon}^{\infty} \\ \left(\mathbf{C}-\mathbf{C}^{(2)}\right)^{-1}\mathbf{C}\left\langle\boldsymbol{\varepsilon}^{*}\right\rangle_{\Gamma_2}-\left\langle\boldsymbol{\varepsilon}^{\mathrm{p}}\right\rangle_{\Gamma_2}=\boldsymbol{\varepsilon}^{\infty} \\ \vdots \\ \left(\mathbf{C}-\mathbf{C}^{(N)}\right)^{-1}\mathbf{C}\left\langle\boldsymbol{\varepsilon}^{*}\right\rangle_{\Gamma_N}-\left\langle\boldsymbol{\varepsilon}^{\mathrm{p}}\right\rangle_{\Gamma_N}=\boldsymbol{\varepsilon}^{\infty} \end{cases} \tag{A.2}$$

Additionally, when the Eshelby tensor of all regions are identical owing to their homothety and confocality, the relationships between the average transformation and perturbation strains of each phase are expressed as follows.

$$\begin{cases} \left\langle \boldsymbol{\varepsilon}^{\mathrm{p}} \right\rangle_{\Omega_1} = \mathbf{S} \left\langle \boldsymbol{\varepsilon}^{*} \right\rangle_{\Omega_1} \\ \left\langle \boldsymbol{\varepsilon}^{\mathrm{p}} \right\rangle_{\Gamma_2} = \mathbf{S} \left\langle \boldsymbol{\varepsilon}^{*} \right\rangle_{\Gamma_2} \\ \qquad \vdots \\ \left\langle \boldsymbol{\varepsilon}^{\mathrm{p}} \right\rangle_{\Gamma_N} = \mathbf{S} \left\langle \boldsymbol{\varepsilon}^{*} \right\rangle_{\Gamma_N} \end{cases} \tag{A.3}$$

Substitution from (A.3) into (A.2) results into following expressions for average transformation strains.

$$\begin{cases} \left\langle \boldsymbol{\varepsilon}^{*} \right\rangle_{\Omega_1} = \left[\left(\mathbf{C} - \mathbf{C}^{(1)} \right)^{-1} \mathbf{C} - \mathbf{S} \right]^{-1} \boldsymbol{\varepsilon}^{\infty} \\ \left\langle \boldsymbol{\varepsilon}^{*} \right\rangle_{\Gamma_2} = \left[\left(\mathbf{C} - \mathbf{C}^{(2)} \right)^{-1} \mathbf{C} - \mathbf{S} \right]^{-1} \boldsymbol{\varepsilon}^{\infty} \\ \qquad \vdots \\ \left\langle \boldsymbol{\varepsilon}^{*} \right\rangle_{\Gamma_N} = \left[\left(\mathbf{C} - \mathbf{C}^{(N)} \right)^{-1} \mathbf{C} - \mathbf{S} \right]^{-1} \boldsymbol{\varepsilon}^{\infty} \end{cases} \tag{A.4}$$

The coefficients behind $\boldsymbol{\varepsilon}^{\infty}$ in the above expressions, hereafter denoted by $\mathbf{H}^{(i)}$, are used in the following equation estimating the effective elasticity of the multilayer inclusion, $\mathbf{C}^{\mathrm{eff}}$.

$$\mathbf{C}^{\mathrm{eff}} = \mathbf{C}\left[\mathbf{I} + \left(\mathbf{S} - \mathbf{I} \right) \mathbf{H}_{\mathrm{R}} \right] \left(\mathbf{I} + \mathbf{S}\mathbf{H}_{\mathrm{R}} \right)^{-1} \qquad \text{where} \qquad \mathbf{H}_{\mathrm{R}} = \sum_{i=1}^{N} f_i \mathbf{H}^{(i)} \tag{A.5}$$

In the above equation, f_i is the volume fraction of phase '*i*' relative to the entire multilayer heterogeneity, and trivially $\sum_{i=1}^{N} f_i = 1$. As a plausible choice of the reference medium which is also suggested in [15], the elasticity of the host medium is set equal to that of the entire heterogeneity, i.e. $\mathbf{C}^{\mathrm{eff}} = \mathbf{C}$. Simultaneous solution of this equality and Eq.(A.5) leads to the following equation which is analogue of Eq.(4.6a) in [15].

$$\mathbf{H}_{\mathrm{R}} = \mathbf{0} \qquad \Rightarrow \qquad \sum_{i=1}^{N} f_i \left[\left(\mathbf{C} - \mathbf{C}^{(i)} \right)^{-1} \mathbf{C} - \mathbf{S} \right]^{-1} = \mathbf{0} \tag{A.6}$$

Given that Eshelby's tensor corresponds the multiplication of polarization tensor, $\mathbf{P}$, and the reference stiffness tensor, this last equation can be further simplified as follows.

$$\left.\begin{aligned}&\mathbf{S}=\mathbf{PC}\\&\sum_{i=1}^{N} f_i\left[\left(\mathbf{C}-\mathbf{C}^{(i)}\right)^{-1}\mathbf{C}-\mathbf{S}\right]^{-1}=\mathbf{0}\end{aligned}\right\}\Rightarrow\quad \sum_{i=1}^{N}\left\{f_i\left[\mathbf{I}-\left(\mathbf{C}-\mathbf{C}^{(i)}\right)\mathbf{P}\right]^{-1}\left(\mathbf{C}-\mathbf{C}^{(i)}\right)\right\}=\mathbf{0} \qquad \text{(A.7)}$$

The above equation, referred to as HNNM equation in this work, is the simplified representation of HNNM description of the effective elasticity of multilayer inclusions where all phases are coaxial and have nearly identical Eshelby tensors. Accordingly, this relationship suits well concentric spheroidal configurations treated in this study. This equation obviously applies to any multiphase ellipsoidal heterogeneity in which all regions share the same Eshelby's tensor such as multilayer spherical particles. From the numerical point of view, Eq.(A.7) is preferable to Eq.(A.6) since the former is singular at all $\mathbf{C}^{(i)}$ whereas in the latter such singularities are removed. Properly speaking, $\mathbf{C}^{(i)} \neq \mathbf{C}$ which is exploited here, is hypothesized by Hori and Nemat-Nasser [15] during the derivation procedure.

Appendix B

Similar to Appendix A, the adapted form of modified HNNM for multiphase inclusions made of concentric phases with identical Eshelby's tensors is formulated. The following arguments are consistent with the relationships presented in [16] which are essentially an extension to the formalism of Hori and Nemat-Nasser [15] and also the improvement proposed by Aboutajeddine & Neale [35]. In this appendix, 'D-S-B:' before any equation number stands for Dinzart, Sabar & Berbenni [16] and refers to the equation from that reference. According to (D-S-B: 40), the effective stiffness of an *N*-phase multi-coating reinforcement embedded in a medium with the boundary conditions of uniform strain at infinity is described as follows

$$\begin{aligned}
&\mathbf{C}^{(\mathrm{eff})} = \mathbf{C}^{(N)} + \sum_{K=1}^{N-1} \left\{ f_K \left(\mathbf{C}^{(K)} - \mathbf{C}^{(N)} \right) \mathbf{A}^{(K/\mathrm{eff})} \right\} \quad \text{where} \quad \mathbf{A}^{(K/\mathrm{eff})} = \frac{1}{f_K} \Delta \mathbf{A}^{(\Omega_K/\Omega_N)} \mathbf{A}^{(\Omega_N/\mathrm{eff})} \\
&\mathbf{A}^{(\Omega_N/\mathrm{eff})} = \left[\mathbf{I} + \mathbf{P}_{\mathrm{eff}}^{(\Omega_N)} \sum_{J=1}^{N} \left(\mathbf{C}^{(J)} - \mathbf{C}^{(\mathrm{eff})} \right) \Delta \mathbf{A}^{(\Omega_J/\Omega_N)} \right]^{-1}
\end{aligned} \tag{B.1}$$

Similar to the numbering convention of HNNM, the outermost phase is numbered '*N*' and the core phase is numbered '1'. Substitution of $\mathbf{A}^{(K/\mathrm{eff})}$ into the expression of $\mathbf{C}^{(\mathrm{eff})}$ gives the following simpler form of representation for the effective stiffness.

$$\mathbf{C}^{(\mathrm{eff})} = \mathbf{C}^{(N)} + \sum_{K=1}^{N-1} \left\{ \left(\mathbf{C}^{(K)} - \mathbf{C}^{(N)} \right) \Delta \mathbf{A}^{(\Omega_K/\Omega_N)} \right\} \mathbf{A}^{(\Omega_N/\mathrm{eff})} \tag{B.2}$$

Here, Ω_J denotes the closed region of space delineated by the outer boundary of phase *J*. Fourth-order strain concentration tensors, $\mathbf{A}$, have the following definitions.

$$\begin{aligned}
&\mathbf{A}^{(\Omega_K/\Omega_{K+1})} = \left\{ \mathbf{I} + \frac{f_{K+1}}{\sum_{L=1}^{K+1} f_L} \mathbf{P}_{K+1}^{(K+1)} \sum_{L=1}^{K} \left(\mathbf{C}^{(L)} - \mathbf{C}^{(K+1)} \right) \Delta \mathbf{A}^{(\Omega_L/\Omega_K)} \right\}^{-1} \\
&\mathbf{A}^{(\Omega_K/\Omega_J)} = \prod_{L=K}^{J-1} \mathbf{A}^{(\Omega_L/\Omega_{L+1})} = \mathbf{A}^{(\Omega_K/\Omega_{K+1})} \mathbf{A}^{(\Omega_{K+1}/\Omega_{K+2})} \cdots \mathbf{A}^{(\Omega_{J-1}/\Omega_J)}
\end{aligned} \tag{B.3}$$

Although the last relationship is not explicitly given in [16] it can be easily deduced from the definition of strain concentration tensors. Note that tensor multiplication is

not, in general, commutative and the above order of multiplication of concentration tensors has to be respected. Additionally, $\mathbf{A}^{(\Omega_L/\Omega_L)} = \mathbf{I}$ and

$$\Delta\mathbf{A}^{(\Omega_L/\Omega_K)} = \left(\sum_{i=1}^{L} f_i\right)\left(\sum_{i=1}^{K} f_i\right)^{-1}\mathbf{A}^{(\Omega_L/\Omega_K)} - \left(\sum_{i=1}^{L-1} f_i\right)\left(\sum_{i=1}^{K} f_i\right)^{-1}\mathbf{A}^{(\Omega_{L-1}/\Omega_K)} \tag{B.4}$$

Note that the expression for $\Delta\mathbf{A}^{(\Omega_K/\Omega_N)}$ in (D-S-B: 44) is not consistent with the corresponding one in (D-S-B: 35). From (D-S-B: 35), it can be easily shown that

$$\Delta\mathbf{A}^{(\Omega_K/\Omega_N)} = \left(\sum_{J=1}^{K} f_J\right)\mathbf{A}^{(\Omega_K/\Omega_N)} - \left(\sum_{J=1}^{K-1} f_J\right)\mathbf{A}^{(\Omega_{K-1}/\Omega_N)} \tag{B.5}$$

which means that the term 'f_K' in the denominator of (D-S-B: 44) is superfluous. Similarly, 'f_K' in the denominator of the expression immediately after (D-S-B: 41) is superfluous. Next, the fourth-order tensor $\mathbf{P}_{J+1}^{(J+1)}$ is expressed as

$$\mathbf{P}_{J+1}^{(J+1)} = \mathbf{P}_{J+1}^{(\Omega_{J+1})} - \frac{\sum_{L=1}^{J+1} f_L}{f_{J+1}}\left(\mathbf{P}_{J+1}^{(\Omega_{J+1})} - \mathbf{P}_{J+1}^{(\Omega_J)}\right) \tag{B.6}$$

where $\mathbf{P}_{J+1}^{(\Omega_J)} = \mathbf{P}\left(\mathbf{C}^{(J+1)}, \Omega_J\right)$ denotes the polarization tensor of region Ω_J with $\mathbf{C}^{(J+1)}$ being its reference stiffness. Obviously, $\mathbf{P}_{J+1}^{(\Omega_J)}$ is related to Eshelby's tensor as follows.

$$\mathbf{P}_{J+1}^{(\Omega_J)} = \mathbf{S}(\mathbf{C}^{(J+1)}, \Omega_J)\left(\mathbf{C}^{(J+1)}\right)^{-1} \tag{B.7}$$

Likewise, $\mathbf{P}_{\text{eff}}^{(\Omega_N)} = \mathbf{P}\left(\mathbf{C}^{(\text{eff})}, \Omega_N\right)$. Having defined all the variables required for estimating $\mathbf{C}^{\text{eff}}$, one can adapt the formulation to the specific configuration of multiphase reinforcements made of concentric and similar ellipsoidal phases in the sense that their Eshelby's tensors are identical. This constraint simplifies Eq.(B.6) in the following way

$$\mathbf{P}_{J+1}^{(\Omega_{J+1})} = \mathbf{P}_{J+1}^{(\Omega_J)} \qquad \Rightarrow \qquad \mathbf{P}_{J+1}^{(J+1)} = \mathbf{P}_{J+1}^{(\Omega_J)} \tag{B.8}$$

Thus, the index of region Ω can be removed as all regions are similar and no distinction between the regions is required. It can be seen that, contrary to HNNM formulation, the constraint of similarity of the ellipsoidal regions allows no further

simplification to the above system of equations. As a simple and straightforward verification, for a two-phase heterogeneity, called 'double-inclusion' in [15] and [35], the expression of $\mathbf{C}^{(\mathrm{eff})}$ is obtained as follows after some mathematical manipulations

$$\mathbf{C}^{(\mathrm{DI})} = \mathbf{C}^{(2)} + f_1 \left\{ \left[\mathbf{I} + \mathbf{P}_{\mathrm{eff}}^{(\mathrm{DI})} \left(\mathbf{C}^{(2)} - \mathbf{C}^{(\mathrm{eff})} \right) \right] \left[\left(\mathbf{C}^{(1)} - \mathbf{C}^{(2)} \right)^{-1} + f_2 \mathbf{P}_2^{(\mathrm{DI})} \right] + f_1 \mathbf{P}_{\mathrm{eff}}^{(\mathrm{DI})} \right\}^{-1} \tag{B.9}$$

which is consistent with the expression derived by Aboutajeddine & Neale [35].

Appendix C

In this appendix, Hashin-Shtrikman bounds for the equivalent moduli of *n*-phase spherical particles are presented. The following development is built on certain equations derived in [36] and [37]. From the former, the general equation defining H-S bounds on the stiffness components of a general *n*-phase composite system in which neither of phases can be identified as the comparison (reference) phase is given by

$$\mathbf{C}^{\mathrm{B}}=\left[\sum_{i=1}^{n} f_i\left[\mathbf{I}+\left(\mathbf{C}^{(i)}-\mathbf{C}^{\mathrm{c}}\right)\mathbf{P}\right]^{-1}\right]^{-1}\sum_{i=1}^{n} f_i\left[\mathbf{I}+\left(\mathbf{C}^{(i)}-\mathbf{C}^{\mathrm{c}}\right)\mathbf{P}\right]^{-1}\mathbf{C}^{(i)} \tag{C.1}$$

This equation is valid only if the shape and distribution polarization tensors are identical, meaning that $\mathbf{P}_{\mathrm{s}}=\mathbf{P}_{\mathrm{d}}=\mathbf{P}$. This is obviously the case of an isotropic, matrix-based composite system containing *n*-1 types of isotropic, spherical particles with randomly uniform distribution. To determine the lower bound $\mathbf{C}^{\mathrm{B}-}$, one needs to build the comparison stiffness, $\mathbf{C}^{\mathrm{c}}$, by choosing the minimal value of each component in $\mathbf{C}^{(i)}$. Analogously, the upper bound $\mathbf{C}^{\mathrm{B}+}$, is constructed by choosing the maximal value of each component in $\mathbf{C}^{(i)}$ to build the associated $\mathbf{C}^{\mathrm{c}}$. Note that since the comparison stiffness is constructed in a componentwise manner, the as-built $\mathbf{C}^{\mathrm{c}}$ might correspond to none of $\mathbf{C}^{(i)}$. Moreover, in deriving Eq.(C.1), no constraint has been placed on the relative position of constituents, which means that it equally applies to the equivalent stiffness of *n*-phase, isotropic, spherical heterogeneities made up of isotropic, spherical phases.

Parnell in [37] employed an efficient convention of short-hand notation in representing fourth-order, isotropic tensors, which is exploited here because in applying Eq.(C.1) to *n*-phase spherical heterogeneity problem under study, all fourth-order tensors are isotropic. Their system of notation simplifies to a great extent the mathematical manipulations involved, as demonstrated in the following. According to this system of notation (cf. Section 5 and Appendix C of [37]), $\mathbf{I}$ is

decomposed into deviatoric, $\mathbf{K}$, and volumetric, $\mathbf{J}$, parts to form an orthonormal tensor basis.

$$\mathbf{I}_{ijkl} = \frac{1}{2}\left(\boldsymbol{\delta}_{ik}\boldsymbol{\delta}_{jl} + \boldsymbol{\delta}_{il}\boldsymbol{\delta}_{jk}\right), \qquad \mathbf{J}_{ijkl} = \frac{1}{3}\left(\boldsymbol{\delta}_{ij}\boldsymbol{\delta}_{kl}\right), \qquad \mathbf{K} = \mathbf{I} - \mathbf{J} \tag{C.2}$$

It can be shown that the adopted decomposition has the following properties.

$$\mathbf{JJ} = \mathbf{J}, \qquad \mathbf{KK} = \mathbf{K}, \qquad \mathbf{KJ} = \mathbf{JK} = \mathbf{0} \tag{C.3}$$

In this orthonormal basis, the fourth-order tensors of interest can be represented in the following short-hand form.

$$\begin{aligned} &\mathbf{C}^{(i)} = 3\kappa_i\mathbf{J} + 2\mu_i\mathbf{K}, \quad \mathbf{C}^{\mathrm{c}} = 3\kappa_{\mathrm{c}}\mathbf{J} + 2\mu_{\mathrm{c}}\mathbf{K} \\ &\mathbf{P} = P_1\mathbf{J} + P_2\mathbf{K} \qquad \text{where} \qquad P_1 = \frac{1}{3\kappa_{\mathrm{c}} + 4\mu_{\mathrm{c}}}, \qquad P_2 = \frac{3\left(\kappa_{\mathrm{c}} + 2\mu_{\mathrm{c}}\right)}{5\mu_{\mathrm{c}}\left(3\kappa_{\mathrm{c}} + 4\mu_{\mathrm{c}}\right)} \end{aligned} \tag{C.4}$$

With this form of representation, the summation, multiplication and inversion operations between fourth-order tensors are performed componentwise. Substitution from (C.4) into Eq.(C.1) yields

$$\begin{aligned} \mathbf{C}^{\mathrm{B}} = &\left[\sum_{i=1}^{n} f_i\left[\mathbf{J} + \mathbf{K} + \left((3\kappa_i - 3\kappa_{\mathrm{c}})\mathbf{J} + (2\mu_i - 2\mu_{\mathrm{c}})\mathbf{K}\right)\left(P_1\mathbf{J} + P_2\mathbf{K}\right)\right]^{-1}\right]^{-1} \times \\ &\sum_{i=1}^{n} f_i\left[\mathbf{J} + \mathbf{K} + \left((3\kappa_i - 3\kappa_{\mathrm{c}})\mathbf{J} + (2\mu_i - 2\mu_{\mathrm{c}})\mathbf{K}\right)\left(P_1\mathbf{J} + P_2\mathbf{K}\right)\right]^{-1}\left(3\kappa_i\mathbf{J} + 2\mu_i\mathbf{K}\right) \end{aligned} \tag{C.5}$$

Further simplification gives

$$\begin{aligned} &\mathbf{C}^{\mathrm{B}} = 3\kappa^{\mathrm{B}}\mathbf{J} + 2\mu^{\mathrm{B}}\mathbf{K} = \\ &\left[\sum_{i=1}^{n}\frac{f_i}{1 + 3\kappa_i P_1 - 3\kappa_{\mathrm{c}}P_1}\mathbf{J} + \sum_{i=1}^{n}\frac{f_i}{1 + 2\mu_i P_2 - 2\mu_{\mathrm{c}}P_2}\mathbf{K}\right]^{-1}\left[\sum_{i=1}^{n}\frac{3f_i\kappa_i}{1 + 3\kappa_i P_1 - 3\kappa_{\mathrm{c}}P_1}\mathbf{J} + \sum_{i=1}^{n}\frac{2f_i\mu_i}{1 + 2\mu_i P_2 - 2\mu_{\mathrm{c}}P_2}\mathbf{K}\right] \end{aligned} \tag{C.6}$$

which finally leads to following scalar equations representing H-S bounds of the equivalent bulk and shear moduli of an *n*-phase spherical heterogeneity.

$$\kappa^{\mathrm{B}} = \left[\sum_{i=1}^{n} \frac{f_i}{4\mu_{\mathrm{c}} + 3\kappa_i}\right]^{-1} \sum_{i=1}^{n} \frac{f_i \kappa_i}{4\mu_{\mathrm{c}} + 3\kappa_i}$$
$$\mu^{\mathrm{B}} = \left[\sum_{i=1}^{n} \frac{f_i}{3\kappa_{\mathrm{c}}\left(3\mu_{\mathrm{c}} + 2\mu_i\right) + 4\mu_{\mathrm{c}}\left(2\mu_{\mathrm{c}} + 3\mu_i\right)}\right]^{-1} \sum_{i=1}^{n} \frac{f_i \mu_i}{3\kappa_{\mathrm{c}}\left(3\mu_{\mathrm{c}} + 2\mu_i\right) + 4\mu_{\mathrm{c}}\left(2\mu_{\mathrm{c}} + 3\mu_i\right)} \tag{C.7}$$

The above development is more general than the bounds derived in [38], in that the comparison material is not required to correspond one of the constituents.